ADVANCES IN INORGANIC CHEMISTRY, VOL. 46

COMING TO GRIPS WITH REACTIVE INTERMEDIATES

ANTHONY J. DOWNS and TIMOTHY M. GREENE

Inorganic Chemistry Laboratory, University of Oxford, Oxford OX1 3QR, United Kingdom

It is a capital mistake to theorise before one has data. Insensibly one begins to twist facts to suit theories, instead of theories to suit facts.

A. Conan Doyle, "A Scandal in Bohemia"

I. Introduction

Chemistry is the science of change. It is ironic then that, although we have become so knowledgeable about the properties of reactants and products—about the beginnings and ends of chemical journeys—we remain more often than not unsure of just how those journeys are made. Our modern armory of sophisticated spectroscopic and diffraction methods provides every expectation of a direct hit on the "fixed" objects represented by reactants and products, but is seldom

0898-8838/99 $25.00

equipped to target the shadowy, moving entity presented by the *process* of their interconversion. How the reaction rate varies with concentration, temperature, and other conditions may give vital clues but rarely establishes with any certainty the mechanism of what may be, at least superficially, quite a simple homogeneous reaction.

Elaborating the mechanism of a reaction is an altogether more complicated undertaking than determining the structures of long-lived reagents or products in that we are seeking ultimately a detailed description of the way in which the structure and bonding of the reagents change with time in each of the several individual acts that normally make up a chemical change. In general terms, a complete account of any such mechanism is going to require knowledge of no less than four aspects (*1–3*):

1. subdivision of the reaction into its individual steps or equilibria;
2. characterization of each intermediate species in terms of its composition, structure, energy states, and lifetime;
3. a description of the transition state appropriate to each elementary reaction step, again with reference to composition, stereochemistry, and energetics; and
4. a complete specification of the processes leading to and from each transition state in relation to the geometries and energy levels (mainly electronic and vibrational) of the reactants, intermediates, and products in their ground and excited states.

With reactions occurring as they usually do in solution, the role of the solvent at each stage needs to be realistically assessed. The history of kinetic studies is littered with the wrecks of mechanistic hypotheses that ultimately foundered on the unsuspected reefs of solvent mediation. It can come as no surprise, then, that a comprehensive mechanistic description is still well beyond the reach of present techniques, both practical and theoretical, except in a few cases, and those mostly confined to the simplest of systems. More often than not we are obliged to piece together a mechanism that is consistent with *all* the available facts, both kinetic and nonkinetic; very rarely do we have compelling and unambiguous evidence of one particular mechanism.

Nothing could be much simpler, it might be thought, than the exchange that the neutral metal hexacarbonyl $Cr(CO)_6$ undergoes with free CO in both the solution and gas phases, particularly as it proceeds in accordance with a rate law of the form

$$-d[Cr(CO)_6]/dt = k_1[Cr(CO)_6].$$

The solvent having little effect on the activation parameters, it is reasonable to assume that a dissociative mechanism is at work, with rate-determining fission of a Cr–CO bond being followed by rapid attack at the resulting pentacoordinated intermediate $Cr(CO)_5$ (*4–6*). Early kinetic studies on substitution of CO by another two-electron ligand L,

$$Cr(CO)_6 + L \rightarrow Cr(CO)_5L + CO \qquad (1)$$

e.g., L = amine, phosphine, or phosphite,

appeared also (*4–6*) to point to a simple dissociative mechanism, again with $Cr(CO)_5$ as a common intermediate. However, investigations extending over a much wider concentration range have now shown that a two-term rate law is commonly applicable, *viz.*

$$-d[Cr(CO)_6]/dt = k_1[Cr(CO)_6] + k_2[Cr(CO)_6][L] \qquad (2)$$

The activation parameters $\Delta H‡$ and $\Delta S‡$ characterizing the k_1 term are very similar to those associated with CO exchange, whereas $\Delta H_2‡$ for the k_2 term is significantly smaller than $\Delta H_1‡$, and $\Delta S_2‡$, being negative, differs not only in magnitude but also in sign from $\Delta S_1‡$. The most plausible interpretation of these and related experiments is that substitution occurs via two competing pathways, one involving a dissociative mechanism closely akin to that envisaged for CO exchange (see Fig. 1), and the other a "dissociative interchange" (I_d)

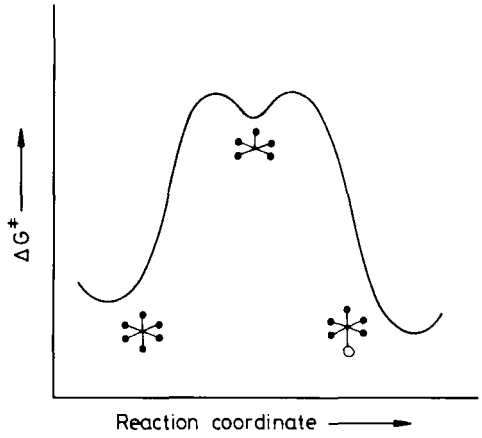

FIG. 1. Hypothetical free energy profile for the substitution reaction $Cr(CO)_6 + L \rightarrow Cr(CO)_5L + CO$ on the assumption that it proceeds via a dissociative mechanism.

process in which there is relatively little bond-making in the transition state. How then are we to picture this I_d process? Perhaps L forms encounter complexes in which it occupies an outer-sphere site of a solvated $Cr(CO)_5$ fragment. There are other possible explanations, though, and we are now on the "tossing sea" of conjecture, however well informed, rather than the firm ground of incontestable result or inference.

Still more problematic is the apparent migratory insertion of nitric oxide into transition metal–carbon bonds, an important reaction in metal nitrosyl complexes and one that may be relevant to biochemical reactions (*7*). On the evidence of isotopic labeling and kinetic experiments, the insertion of NO into the Co–CH_3 bond of the (cyclopentadienyl)cobalt complex (η^5-C_5H_5)Co(NO)(CH_3), which occurs in Reaction (*3*),

$$(\eta^5\text{-}C_5H_5)Co(NO)(CH_3) + PPh_3 \rightarrow (\eta^5\text{-}C_5H_5)Co(PPh_3)[N(O)CH_3], \quad (3)$$

is intramolecular, and the experimental results are consistent with, but do not prove, a mechanism involving methyl migration, followed by phosphine addition (see Scheme 1, lower path) (*8*). This has the attraction of resembling the mechanism generally agreed to hold for CO insertion in a reaction such as

$$Mn(CO)_5CH_3 + CO \rightarrow Mn(CO)_5[C(O)CH_3] \quad (4)$$

and which is a critical step in many important carbon–carbon bond-forming processes mediated by homogeneous transition-metal cata-

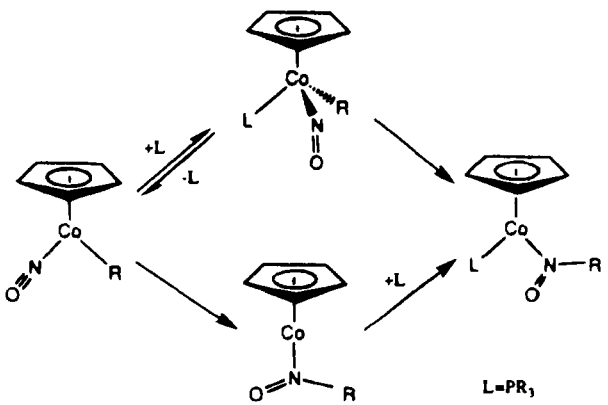

SCHEME 1. Alternative pathways for the migratory insertion reaction of (η^5-C_5H_5)Co(NO)(CH_3) in the presence of a phosphine (*8*).

lysts. Still, the worm of doubt may turn. For is not NO a more versatile ligand than CO, and can it not, for example, function as either a $3e^-$ ligand or a $1e^-$ ligand? Thus, addition of a phosphine molecule accommodated by a change in the ligation of the NO to give a bent Co–N–O unit offers another reaction pathway, as shown by the upper route in Scheme 1. There is persuasive evidence that such a change affords a low-energy channel in other reactions (*8*), and it is not obvious why it should not do so to effect NO insertion. In the absence of any definitive experimental information on this score, quantum chemical calculations have been carried out to explore each of the two possible pathways (*8*). The geometries and energies of the reactants, intermediates, transition states, and products have been determined on the basis of Density Functional Theory (DFT), with the results illustrated in Fig. 2. Hence it emerges that the mechanism in which NO insertion precedes phosphine association incurs activation barriers not exceeding 84 $kJ \cdot mol^{-1}$ and is therefore favored over the mechanism involving insertion *after* phosphine addition, which is opposed by appreciably higher barriers (80–218 $kJ \cdot mol^{-1}$). This pleasing endorsement by theory of the mechanism deduced by experiment may seem to settle the issue, but the theory has not been able to budget for the effects of solvation. Still, we cannot be entirely sure of our ground, and about this particular reaction the last word has surely not been said.

The preceding examples of CO exchange and NO insertion reactions have to do with systems that have attracted considerable experimental and theoretical attention. Accordingly, although there are fundamental questions still to be answered, some mechanistic features at least are not in doubt. For most of the myriad chemical reactions that

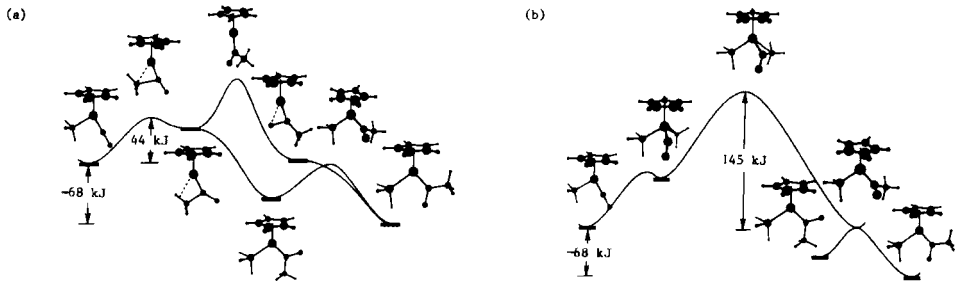

FIG. 2. The calculated profiles of the potential energy surfaces (at the DFT-B3LYP level) for the insertion reaction (η^5-C_5H_5)Co(NO)(CH_3) + phosphine → (η^5-C_5H_5)Co(phosphine)[N(O)CH_3] on the assumption (a) of an intramolecular rate-determining mechanism, or (b) of an associative mechanism (*8*).

are known to occur, though, we have neither the facts nor the theory to argue the mechanistic case, and analogy and intuition may well be the sole guiding principles. Hence we may be spared the great tragedy of science—that is, the "slaying of a beautiful hypothesis by an ugly fact"—but, without a secure understanding of mechanism, we are hostages to experience, empiricism, and prejudice when it comes to devising the most efficient, safe, and reliable way of engineering a desired chemical change.

II. Reaction Intermediates: Nerve Centers of Chemical Reactions

Crucial to any problem of mechanism must be the part played by any intermediate compound, for example (i) $Cr(CO)_5$ in the exchange reactions of $Cr(CO)_5L$ (L = CO or other ligands) and (ii) either $(C_5H_5)Co[N(O)CH_3]$ or $(C_5H_5)Co(phosphine)(NO)(CH_3)$ in Reaction (3). Indeed, were it possible to detect, identify, and characterize the relevant intermediates, the primary issue of which path is taken in Reaction (3) (see Scheme 1) could be settled beyond peradventure. More generally, the intermediates may be open-shell molecules; they may be radicals; they may involve elements in unusual oxidation states or with unusual coordination geometries or partners. However, until we know what these intermediates are and the part they play, we cannot begin to comprehend the mechanism of any given reaction. As a start, we need to be sure of not only the identities but also the molecular and electronic structures of the intermediates. Such properties cannot necessarily be deduced from the properties of stable molecules and may well challenge conventional principles of bonding. This is all very well, but how are we to cope with intermediates that have but a fleeting existence under normal conditions? At a vapor pressure of 1 torr and in the presence of CO, for example, $Cr(CO)_5$ is found to have a lifetime in the order of one-millionth of a second at room temperature (*9*).

To counter the all too brief stay normally enjoyed by a molecule such as $Cr(CO)_5$, the experimenter has three main options. One way is to slow down or inhibit the reactions disposing of the molecule. Another is to record a spectroscopic autograph, in absorption or emission, within the lifetime of the transient and so monitor its temporal fate (as in "flash photolysis"). The third is to resort to a flow method, depending on continuous generation of the intermediate in a fluid traveling at a uniform rate along a tube; under the right conditions, decay of the intermediate gives rise to a steady-state concentration

that varies as a function of the distance traveled along the tube, and that may be analyzed by essentially "static" spectroscopic measurements. Each method has its strengths and weaknesses. None is able individually to deliver all the information we are likely to require for a proper appreciation of how the intermediate fits into the overall mechanism of a given reaction. If we are to realize that ambition, we must be looking therefore to exploit not one but several methods.

To gain a better idea of the three strategies for characterizing short-lived intermediates—namely, retardation, time-resolved, or flow methods—we turn next to a brief survey of how they work in practice and of just what light they can or cannot shed on a particular intermediate. How mechanistic studies have been advanced in this way will be illustrated in the course of the account.

III. Experimental Characterization of Reaction Intermediates: Retardation

There are various ways of slowing down or even suppressing totally the reactions of a molecule. In principle, we may limit its collisions with other molecules by confining it to the gas phase and there minimizing its pressure; we may minimize the thermal energy to which it has access by lowering its temperature; or we may trap it with a suitable substrate. The best policy in practice may well be either simultaneously or in separate experiments to apply more than one of these restraints.

A. Gas-Phase Studies at Low Pressure

The gas phase at low pressures is the best medium for detailed structural and spectroscopic studies of very simple, robustly bound molecules such as AlH, SiO, or ClO (*10*). Generated typically by thermal or discharge reactions, these may survive at partial pressures high enough and for times long enough to be interrogated by their electronic emission, laser-induced fluorescence, microwave, or infrared absorption spectra, such studies being greatly facilitated by the development of tunable lasers and double resonance techniques. Hence an immense effort has been invested over the years in measuring and analyzing the electronic spectra of stable and unstable diatomic molecules, to give a rich return on information about the bond lengths and vibrational and electronic properties that characterize not only their electronic ground states but also their excited states.

A good example is the molecule SiO, a cosmic precursor to silicon oxide chemistry as we now know it on earth (*11*). In more recent times, too, this molecule has assumed considerable significance because of its relevance to oxidation reactions taking place at the surfaces of silicon wafers and to the creation of antireflection coatings on these and other solid-state devices. Unlike its more familiar counterpart carbon monoxide, SiO is normally quick to aggregate and disproportionate [Reaction (5)] at temperatures below 1000°C:

$$2SiO \rightleftharpoons Si + SiO_2. \tag{5}$$

Stability is not a problem at high temperatures, though, and Reaction (5) can be reversed to produce SiO vapor at a concentration sufficient for microwave absorption measurements by heating a homogeneous mixture of silicon and silicon dioxide to 1350°C in a ceramic reaction vessel, which also serves as the spectroscopic sample chamber (*12*). Alternatively, excited SiO molecules, produced by the action of a discharge on a gaseous mixture including, say, $SiCl_4$ and O_2, can be characterized by their electronic emission spectrum. It has taken 10 to 20 years to unravel all the features of the electronic spectrum extending from the near- to the vacuum-ultraviolet and assign the different band systems, but we now have a relatively full knowledge of the molecule in its electronic ground and numerous excited states (*13*). Rather easier to decipher is the microwave spectrum of the molecule in its electronic ground state, whence a wide range of vibrational and rotational states have been accurately detailed (*11*). These and other studies give every confidence that we are dealing with a $^{28}Si^{16}O$ molecule having the following equilibrium parameters: r_e = 150.9739 pm, ω_e = 1241.56 cm^{-1}, and μ_e = 3.0882 D (*13*). Some of the microwave lines have served as distinctive signatures by which SiO has been recognized in astronomical sources, and SiO masers have relayed important information about both the conditions in circumstellar shells and the mechanisms of mass loss.

Solid boron nitride is a ceramic material of some consequence that can be formed at high temperatures by the reaction of boron atoms with N_2 or NH_3. A likely intermediary in its formation is another high-temperature molecule BN, first observed through its electronic emission spectrum nearly 60 years ago but the properties of which have emerged only slowly (*14*). Identification of the several low-lying electronic states of the molecule is a major problem and only very recently has it become clear that the ground state is not $^1\Sigma^+$ (as with the isoelectronic C_2 molecule) but $^3\Pi$ (*15*). The $A^3\Pi_i$–$X^3\Pi_i$ transition,

the equivalent of the celebrated Swann bands of C_2, can be excited in emission by the action of a microwave discharge on traces of BCl_3 and N_2 entrained in a helium gas stream. Analysis of the well-resolved rotational lines of the 0-0 and 1-0 bands yields the following properties for the ground state of $^{11}B^{14}N$: r_e = 132.9 pm and ω_e = 1514.6 cm^{-1} (*13*, *16*).

The molecule ClO is another reactive species that has attracted still more attention. It plays a significant role in the destruction of stratospheric ozone through catalytic cycles involving heterogeneous and homogeneous reactions, as in Eq. (6) (*17*):

$$\left.\begin{aligned} Cl + O_3 &\rightarrow ClO + O_2 \\ ClO + O &\rightarrow Cl + O_2. \end{aligned}\right\} \qquad (6)$$

Current wisdom can be summarized in the flow chart of Fig. 3. More specifically, the ClO radical is involved in several possible kinetic mechanisms linking global release of chlorofluorocarbons (CFCs) to the Antarctic ozone loss during each austral spring (*18*). An accurate characterization of the spectroscopic and other properties of ClO is therefore vital, not least as a prelude to tracing the crucial correlation between CFCs, ClO, and O_3. ClO is short-lived at the high molecular concentrations characteristic of the condensed phases but can be generated at low pressures in the gas phase, for example by the action of

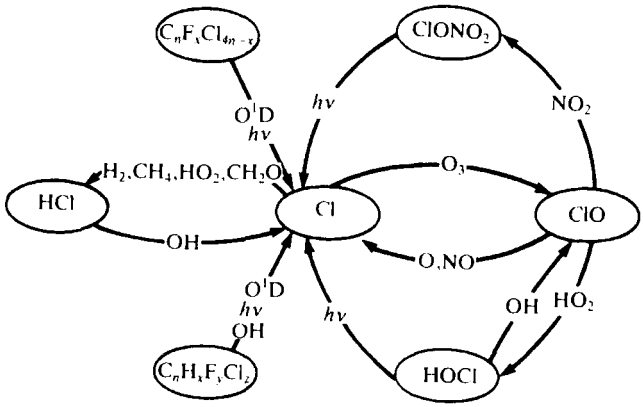

FIG. 3. Chemical cycles affecting the formation and decay of chlorine oxide trace species in the earth's atmosphere (reproduced with permission from Wayne, R. P. "Chemistry of Atmospheres," 2nd ed., p. 137, Clarendon Press: Oxford, 1991).

a microwave discharge or a short burst of radiation on a mixture of Cl_2 and O_2. On the evidence of a detailed analysis of the $A^2\Pi_i$–$X^2\Pi_i$ band system as measured both in absorption and in emission at high resolution, of the infrared spectrum also measured at high resolution, and of the microwave spectrum, the $^{35}Cl^{16}O$ molecule has a $^2\Pi$ ground state with r_e = 156.960 pm, ω_e = 853.724 cm^{-1}, μ_e = 1.24 D, and D_0° = 265.4 $kJ \cdot mol^{-1}$ (*13, 19*). Of its reactivity, though, the properties give the barest hint.

Simple polyatomic molecules such as BH_2 (*20*), BH_3 (*21*), and HBNH (*22*) may be no less amenable to high-resolution spectroscopic studies. Commonly invoked as an intermediate in reactions of boron hydrides, the BH_3 molecule is made elusive by its rapid dimerization to diborane. It is produced, nevertheless, by the action of a dc discharge on a gas stream composed of diborane and helium flowing through a multipass absorption cell; here it can be recognised by its ν_2 (a_2'') and ν_3 (e') vibrational bands as recorded with a high-resolution FT-IR spectrometer (*21*). Detailed analysis of the rotational structure associated with the bands fixes a regular planar D_{3h} structure for BH_3 in its ground electronic state with r_0(B–H) = 119.001 pm. Another discharge reaction, this time involving diborane and ammonia, generates the species HBNH with a lifetime of a few hundred ms under normal conditions. That this is a linear molecule is made clear by the rotational structure of the ν_3 band (corresponding to the BN stretching fundamental) exposed by an IR diode laser spectrometer (*22*); the observed rotational constants imply a BN bond length (123.81 pm) appreciably shorter than those in H_3BNH_3, H_2BNH_2, and even BN itself (165.76, 140.3, and 132.9 pm, respectively).

In principle, electron diffraction is another tool capable of giving precise information about the structure of a gaseous intermediate, even when this is quite a complicated molecule (*23*). In practice, though, there are numerous complications liable to militate against electron diffraction as the sole agency of characterization. Chief among these is the low resolution of the electron-scattering pattern of a molecule. As a result it is seldom easy to discover much about the structure—sometimes even the identity—of a specific molecule in a gaseous mixture. To resolve an otherwise severely underdetermined problem, we need independent testimony about the molecules making up the mixture, for example by reference to the mass, rotational, or vibrational spectrum of the sample or to the results of quantum chemical calculations (*24*). A good example of this strategy is provided by a careful study of the thermal decomposition of trimethylamine vapor (*25*). Mass spectrometric analysis of the vapor stream shows that de-

composition proceeds at 515°C primarily in accordance with Eq. (7) to give methane and the short-lived compound $CH_3-N=CH_2$:

$$(CH_3)_3N \rightarrow CH_4 + CH_3-N=CH_2. \quad (7)$$

Analysis of the electron-diffraction pattern of the reaction mixture implies the following mole fractions: $(CH_3)_3N$, 0.63; CH_4, 0.18; and $CH_3-N=CH_2$, 0.19. The structure of the $CH_3-N=CH_2$ molecule has then been determined by a joint analysis of the electron-diffraction pattern and the rotational constants (derived from the microwave spectrum), giving parameters [$r_Z(N=C)$ = 127.9 pm, $r_Z(N-C)$ = 145.8 pm, and $\angle C-N=C$ = 116.6°] very close to those calculated by *ab initio* methods. Similarly, pyrolysis of propylenimine, $HNCH_2CHCH_3$, at 470°C results in complete decomposition to give the short-lived species *syn-* and *anti*-$CH_3-NH-CH=CH_2$ and *trans*-$CH_3-N=CH-CH_3$ (*26*); geometrical structures and mole fractions of all three products have been deduced by analyzing the electron diffraction pattern of the vapor in concert with the properties implied by quantum chemical calculations. How the proportions of the transients vary with temperature sheds significant light on the reaction path taken by the thermal rearrangement. Life is altogether simpler with only one molecular species in the vapor, and electron diffraction is well established as a primary method of characterizing high-temperature molecules such as $MgCl_2$ (*27*) or C_{70} (*28*). In general, however, the optimum conditions can be met only for a relatively long-lived intermediate such as S_2F_4. This is formed by the dimerization of SF_2 on the winding reaction path that starts with SCl_2 and a metal fluoride and affords the best known route to SF_4, represented mainly by the overall reaction,

$$3SCl_2 + 4MF \rightarrow SF_4 + S_2Cl_2 + 4MCl. \quad (8)$$

(e.g., M = Na or K)

The labile molecule has required the combined forces of electron diffraction, microwave, vibrational, and ^{19}F NMR spectroscopy, and *ab initio* calculations before yielding the secrets of its remarkable, unsymmetrical structure, **I** (*29*); this can be viewed as a trigonal bipyramid centered on one sulfur atom with a lone pair of electrons, the SF group, and one fluorine atom occupying the equatorial sites. Electron-diffraction studies have also contributed to our understanding of how

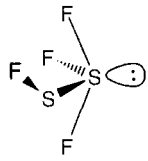

I

gaseous organometallic compounds can, through their decomposition, furnish solid materials with useful electronic or other properties. For example, thermal decomposition of *t*-butylgallium sulfide, $[(Bu^t)GaS]_4$, results in the growth of a new cubic phase of GaS. Not only is this material ideal for the electronic passivation of GaAs surfaces, it has a large band gap, which makes it suitable as the insulating "gate" layer in certain transistor devices. What is striking about the structure of the gaseous precursor, **II**, as determined by electron diffraction, is the presence of a distorted cubane-like Ga_4S_4 core with a *t*-butyl group bound to each gallium atom and *T* symmetry overall (*30*). Irradiation of the precursor with the output of a UV excimer laser gives rise to the photofragments $(Bu^t)_xGa_4S_4$ (where $x = 0–3$), which can be detected by their time-of-flight mass spectra following ionization by a second UV excimer laser. It appears, then, that fragmentation proceeds primarily by loss of the organic substituents with retention of the Ga_4S_4 core, clearly suggesting that growth of cubic GaS depends on the oligomerization of preformed Ga_4S_4 fragments.

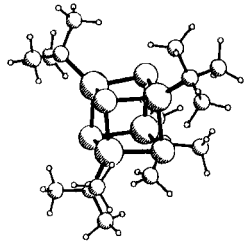

II

Problems of analysis apart, experiments of this sort can at their best provide a remarkably full picture of a gaseous molecule, at least with regard to its *physical* character (*10*). By deliberately seeking to

frustrate any chemical reactions, however, we are naturally denying ourselves any detailed chemical and, in particular, kinetic information. There are other limitations, too. The conditions are far removed in terms of molecular concentrations, as well as environment, from those normally prevailing in the condensed phases. For reasons of rotational congestion, moreover, high-resolution spectroscopic measurements cannot usefully be applied to molecules containing more than a few atoms, and for reasons of pressure and temperature such experiments may lose sight of molecules incorporating weak bonds. In fact, weakly bound molecules commonly feature as the initial products when two reagent molecules interact. These problems lead naturally to the question, How can the power and precision of modern high-resolution spectroscopic methods be brought to bear on larger and/or weakly bound transients? Fast freezing in one form or another is the obvious response.

B. Gas-Phase Studies in Supersonic Jets

When a noble gas seeded with a small amount of other molecules expands through a nozzle into a vacuum, rapid adiabatic cooling occurs, provided that the mean free path of the molecules in the unexpanded gas is short compared with the nozzle diameter. Within only a few nozzle diameters (usually *ca.* 5 mm), the molecules in the jet of gas emerging from the nozzle achieve a very narrow distribution of speeds in the jet direction, clustered around the supersonic value of *ca.* 5×10^4 cm $\cdot$ s^{-1}, and have nearly zero relative speed in directions transverse to this. Consequently, within 5 to 10 μs of emerging from the nozzle into the vacuum, the molecules are in an essentially collisionless state and have a velocity distribution in the transverse direction corresponding to temperatures of a few Kelvin. A similar effective temperature is also achieved through cooling of the rotational and vibrational degrees of freedom. If we can arrange for the intermediate to be formed within the noble-gas stream just before it emerges from the nozzle, freezing times in the order of microseconds can be attained, and thereafter the intermediate is effectively isolated, having no mechanism, either unimolecular or bimolecular, by which to react or decompose. One experimental arrangement, illustrated in Fig. 4, consists of two concentric, coterminal tubes (*31–33*). One reagent admixed with an excess of noble gas is delivered in short pulses via the outer tube while the second reagent (typically also diluted with noble gas) flows continuously through the central tube. The two reagents

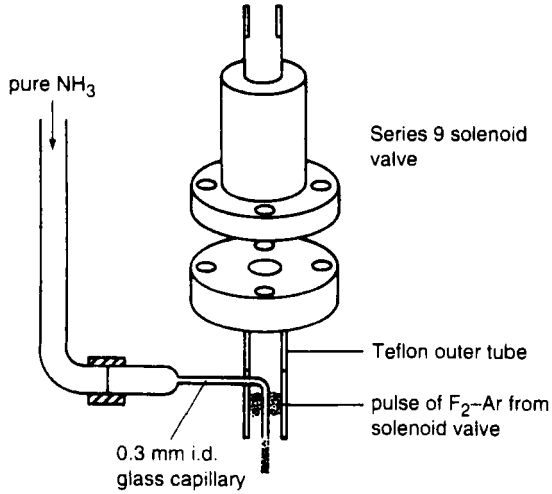

FIG. 4. The fast-mixing nozzle used to observe the rotational spectrum of the gaseous complex $H_3N{\cdots}F_2$ [reproduced with permission from (*33*), p. 112].

meet and mix in the roughly cylindrical interface between the concentric flows as they simultaneously expand. Any intermediate formed here rapidly undergoes collisionless expansion, is then effectively frozen, and may be investigated by such techniques as microwave, infrared diode-laser, laser-induced fluorescence, or photoionization spectroscopy.

For characterizing a dipolar molecule in its electronic ground state, few methods are more instructive than pulsed-nozzle Fourier-transform microwave spectroscopy (*32*). As illustrated schematically in Fig. 5, a short pulse of microwave radiation directed at the gas pulse excites a rotational transition in the species of interest; subsequently the rotationally excited molecules reemit radiation, which is detected. This technique provides a remarkably sensitive probe for transients, the properties of which can be specified with all the precision and detail peculiar to rotational spectroscopy only microseconds after their production. In relation to a weakly bound adduct A···B formed by two molecular reagents A and B, for example, we may draw on the rotational spectrum to determine such salient molecular properties as symmetry, radial and angular geometry, the intermolecular stretching force constant and internal dynamics, the electric charge distribution, and the electric dipole and quadrupole moments of A···B (see Table I).

The mechanism of the addition of molecular chlorine to an alkene

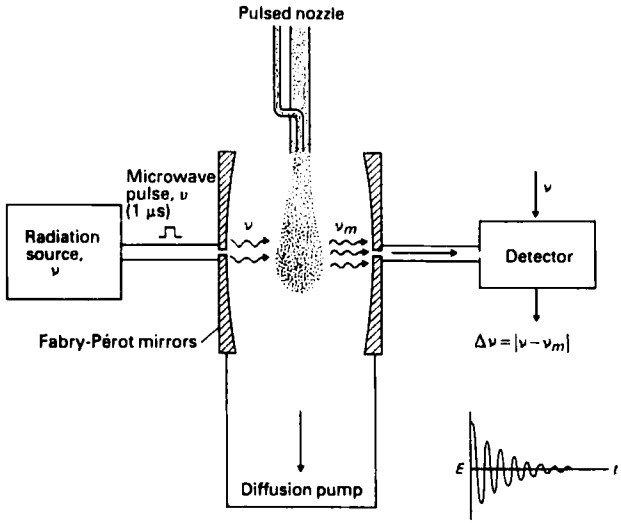

FIG. 5. Pulsed-nozzle FT microwave measurements. A molecule–radiation interaction occurs when the gas pulse is between mirrors forming a Fabry–Pérot cavity. If the transient molecule has a rotational transition of frequency ν_m falling within the narrow band of frequencies carried into the cavity by a short pulse (ca. 1 μs) of monochromatic radiation of frequency ν, rotational excitation leads to a macroscopic electric polarization of the gas. This electric polarization decays only slowly (half-life $T_2 \approx 100$ μs) compared with the relatively intense exciting pulse (half-life in the cavity $\tau_c \approx 0.1$ μs). If detection is delayed until *ca.* 2 μs after the polarization, the exciting pulse has diminished in intensity by a factor of *ca.* 10^6 but the spontaneous coherent emission from the polarized gas is just beginning. This weak emission can then be detected in the absence of background radiation with high sensitivity. For technical reasons, the molecular emission at ν_m is mixed with some of the exciting radiation ν and detected as a signal proportional to the amplitude of the oscillating electric vector at the beat frequency $\nu - \nu_m$ as a function of time, as in NMR spectroscopy; Fourier transformation leads to the frequency spectrum [reproduced with permission from (*31*), p. 563].

has been the subject of much investigation and discussion (*34*). In a fairly polar solvent and in the dark, the reaction has been shown to be of first order in both components, indicating that the entity responsible for electrophilic attack on the alkene is the dihalogen molecule. There is a general consensus that the mechanism, as represented by Eq. (9), involves a pre-equilibrium molecular association of the alkene and Cl_2 to give the adduct **III**:

$$\underset{}{\text{alkene}} + Cl_2 \rightarrow \underset{\textbf{III}}{\text{alkene}\cdots Cl_2} \rightarrow \underset{\textbf{IV}}{\text{alkene}Cl^+} + Cl^- . \qquad (9)$$

TABLE I

MEASURABLE SPECTROSCOPIC AND MOLECULAR PROPERTIES OF GASEOUS A···B MOLECULES ACCESSIBLE THROUGH GROUND-STATE ROTATIONAL SPECTRA (*32*)

Spectroscopic parameter	Molecular property of A···B	Comment/example
Form of the spectrum	Symmetry	Spectral pattern varies for linear, symmetric-top, and asymmetric-top species, e.g., F_2···NH_3 is a symmetric top (*35*).
Rotational constants, A_0, B_0, C_0	Quantitative determination of radial and angular geometry; nature of intermolecular binding	e.g., C_2H_4···Cl_2 (*34*) and F_2···NH_3 (*35*)
Centrifugal distortion constant, D_J or Δ_J	Quadratic force constant for A···B stretching, k_σ	D_J is roughly proportional to k_σ.
Hyperfine coupling constants, χ_{gg} and D_{gg}	Relate to electric field gradient q_{gg}^X at a nucleus X having a nonzero electric quadrupole moment	q_{gg}^X depends on the detailed electric charge distribution within A···B.
Stark effect	Electric dipole moment of A···B	e.g., $HC^{15}N$···$H^{35}Cl$ (*36*)
Zeeman effect	Molecular g factor and electric quadrupole moment of A···B	e.g., Ar···HCl (*37*)

This intermediate then ionizes in the rate-controlling step to give a cation, **IV**, which reacts rapidly with Cl^-. For many years, however, the precise nature of the pre-equilibrium complex **III** has been a matter of speculation. It is clearly desirable to establish with certainty and precision the existence of any such complex. Mixing ethene and molecular chlorine in an apparatus of the type described gives rise to a new ground-state rotational spectrum attributable to the complex C_2H_4···Cl_2. Analysis of the spectrum indicates that this complex has the C_{2v} geometry illustrated in Fig. 6(a), with the Cl_2 molecule lying along the C_2 axis of ethene that is perpendicular to the molecular plane. The weakness of the interaction between the molecules is made abundantly clear by the following features (*34*): the rotational constant A_0 is only slightly larger than the constant C_0 of free ethene; the inner Cl atom is relatively remote from the center of the ethene C=C bond (estimated distance 312.8 pm); at 5.9 $N \cdot m^{-1}$ the intermolecular stretching force constant, k_σ, deduced from the centrifugal distortion

constant is quite minuscule; and the nuclear quadrupole coupling constants $\chi_{gg}(^{35}Cl)$ undergo quite minor changes, implying that the cylindrical symmetry of the electric charge distribution of Cl_2 is only slightly perturbed on complex formation. Hence, there can be little doubt that the intermediate is formally a $b\pi \cdot a\sigma$ complex of the weak, outer type, according to Mulliken's classification.

More complicated and less easily controlled is the reaction between ammonia and fluorine gases, which under normal conditions of temperature and pressure results in a spectacular flame and the formation of NF_3 in small yield. Despite the prodigious reactivity of molecular fluorine, it has proved possible through the device of fast mixing and cooling of the gases in a supersonic jet to detect and characterize the weakly bound prereactive intermediate $H_3N{\cdots}F_2$ on the basis of its ground-state rotational spectrum (*35*). The results attest to the C_{3v} structure illustrated in Fig. 6(b) with a long intermolecular contact, $r(N{\cdots}F)$, of 270.8 pm and a stretching force constant k_σ of no more than 4.7 $N \cdot m^{-1}$. By contrast, the corresponding complex $H_3N{\cdots}ClF$ features an appreciably stronger intermolecular bond, with $r(N{\cdots}Cl)$ = 237.6 pm and k_σ = 34.3 $N \cdot m^{-1}$, pointing to a small but significant transfer of charge in the sense $H_3N{\cdots}Cl^+F^-$ (*38*).

It is not just loosely bound complexes that can be specified with profit by spectroscopic analysis of a supersonic jet. Of this there is no more thrilling example than the transient organometallic radical VCH (*39*), formed when vanadium atoms generated by laser ablation are entrained in a pulse of high-pressure helium containing 5–10% CH_4 prior to expansion to give a supersonic, cooled molecular beam. High-resolution studies of the molecular fluorescence near 800 nm excited by a tunable probe laser reveal extensive vibrational and

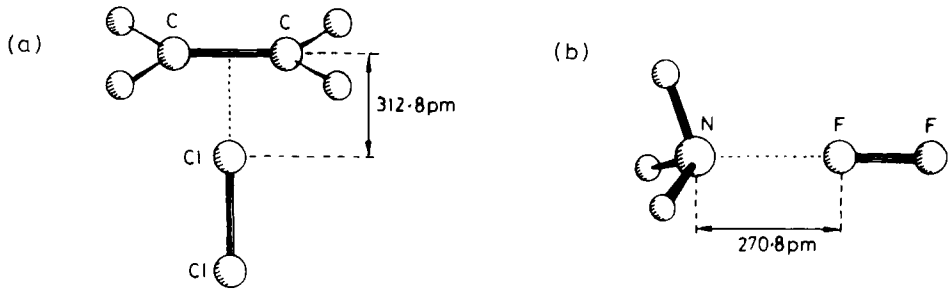

FIG. 6. Structures of the gaseous prereactive intermediates (a) $C_2H_4{\cdots}Cl_2$ and (b) $H_3N{\cdots}F_2$.

rotational detail. Hyperfine patterns characteristic of a nucleus with spin $I = 7/2$ confirm that the carrier contains a vanadium atom; the subband structures are those of a linear molecule; the integer rotational quantum numbers point to an even number of unpaired electrons; and the presence of hydrogen is borne out by experiments with CD_4, which give rise to the corresponding bands of VCD. The ground state of the molecule can be identified unambiguously as $^3\Delta_1$ and the associated rotational constants imply the following dimensions for the substitution structure: $r_S(V{\equiv}C) = 170.2_5$ and $r_S(C{-}H) = 108.0$ pm. Hence, we now have substantive experimental data for an exemplar of the simplest possible type of metal carbyne complex, making clear *inter alia* that the V≡C stretching mode is at 838 cm^{-1}, and not near 1300 cm^{-1} as has been suggested for related species.

Even more challenging are some of the neutral and charged species that are created and destroyed within an electric discharge. Yet, by subjecting a pulsed molecular beam to the combined actions of supersonic expansion and a corona discharge (on the downstream side of the nozzle), it has been possible to detect and study short-lived intermediates as varied as OH, N_2^+, and CH_3 (*40*). Optical spectroscopy has been the traditional source of information, but major contributions to our limited knowledge of the highly complex chemistry of plasmas have come recently from mass, microwave, and infrared laser spectroscopies. Lifetime is not the only problem, for even within the discharge the concentrations of the relevant species are often very small. This has stimulated the development of special modulation techniques to improve both selectivity and sensitivity (*40*). Use of an ac discharge gives, for example, Doppler shifts of spectroscopic frequencies due to molecular ions, which vary with the discharge frequency ν_f, and state populations of any transient species, which vary with twice this frequency. When the spectroscopic detection system is referenced to the frequency ν_f or $2\nu_f$, the resulting demodulated signal consists only of what are velocity-modulated or population-modulated lines, respectively.

Transients such as OH and CH_3 are no mere scientific curiosities—will-o'-the-wisps peculiar to the elaborate combination of discharge, supersonic expansion, and spectroscopic subterfuge. Some of these molecules play vital roles in regimes seemingly quite remote from plasma chemistry. For example, the OH radical is crucially significant as an oxidizing initiator in combustion and in the troposphere, where its natural concentration is liable to be seriously augmented as a re-

sult of pollution (*17*). Two lines of investigation must suffice to demonstrate the scope of modern discharge experiments.

1. The molecules HCCCS and HCCCCS have been characterized by their microwave spectra following their generation by the action of a pulsed discharge on a supersonic molecular beam of argon containing traces of C_2H_2 and CS_2 (*41*). The microwave frequency, swept in small steps of a few MHz, is fed to a Fabry–Pérot cavity, which is maintained at the resonance frequency by synchronous length adjustment so as to retain the high Q value of the cavity. This feature, combined with cooling to rotational temperatures near 1–2 K, enhances greatly the sensitivity of the experiment. The resulting high-resolution spectra are noteworthy for their disclosure that both HCCCS and HCCCCS, in common with HCCS, are linear in their electronic ground states ($^2\Pi$) and so contrast with molecules in the analogous family HC_nO (n = 2–4), all of which are terminated by angular C–C–H units (*41*). That molecules of both series are created in discharge reactions is of more than terrestrial note, because they are potential players of some significance on the interstellar scene.

2. Silane discharges are of practical use as sources of thin-surface films. Infrared diode laser spectroscopy with Zeeman modulation has been exploited to detect and analyze the bending fundamental ν_2 of the pyramidal SiH_3 radical (*42*), which appears to be a primary component of silane plasmas and is likely therefore to be a key intermediate in chemical vapor deposition processes originating in silane. Analysis of the results gives r(Si–H) = 146.8 pm and $\angle$H–Si–H = 110.5°. Other discharge products include SiH_2 and the novel molecule Si_2H_2, which is predominant in a low-pressure silane/argon plasma on the evidence of mass spectrometric measurements. With a low-power plasma cooled at liquid nitrogen temperature, Si_2H_2 can be detected by its submillimeter-wave rotational spectrum. The rotational lines are unaffected by a confining magnetic field and so cannot arise from a paramagnetic or ionic species. Moreover, they correspond to the pattern expected for a near-prolate symmetric top with $(B + C)/2$ = *ca.* 7.2 GHz, a value close to what would be expected for a molecule containing two Si atoms, and adjacent lines exhibit a 3 : 1 intensity alternation consistent with the nuclear spin statistics associated with two equivalent protons. Putting this and other evidence together leads to the double hydrogen-bridged butterfly structure depicted in Fig. 7(a), quite unlike the familiar linear configuration of C_2H_2 (*43*). Confirmation that this is indeed the most stable conformer of Si_2H_2 comes from

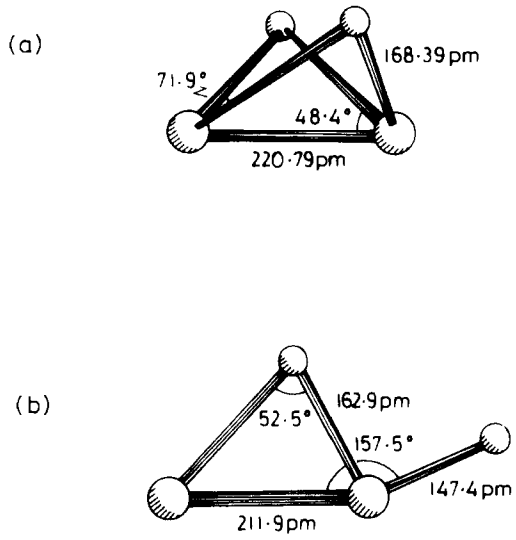

FIG. 7. Structures of the molecule Si_2H_2 present in a silane/argon plasma (a) in its ground electronic state and (b) in an excited state. Dimensions are those determined by analysis of the high-resolution rotational spectra (*43*, *45*).

ab initio quantum chemical calculations (*44*), which also predict, however, the existence of two other stable conformers, including one having the monobridged structure shown in Fig. 7(b) and lying only about 36 $kJ \cdot mol^{-1}$ above the global minimum. It has been a triumph for theory that such a conformer should now have been detected and characterized experimentally following closer scrutiny of the millimeter- and submillimeter-wave rotational spectrum associated with the products of the silane/argon plasma (*45*). The rotational constants of the normal and perdeuterated versions of the molecule afford an r_0 structure with the dimensions indicated in Fig. 7(b) and in tellingly close agreement with those predicted by the *ab initio* calculations. Interestingly, the molecule, which is estimated to have a lifetime not exceeding 10 ms, displays the shortest Si—Si bond to be observed to date. Nor is this the end of the tale, for the heteronuclear species $SiCH_2$, produced by striking an electric discharge in a high-pressure argon pulse seeded with tetramethylsilane vapor, has for its ground state the silylidene structure $Si{=}CH_2$. The molecule has been characterized not only by its microwave spectrum but also by its distinctive, intense laser-induced fluorescence spectrum (*46*), which consists of

15–20 vibronic bands in the 300- to 342-nm region; the rotational structure of the bands, clearly defined at high resolution, features a central subband that is weaker than the outer ones, a necessary consequence of the nuclear statistical weights if there are two equivalent hydrogen atoms. The rotational constants of $SiCH_2$ and $SiCD_2$ have been used to deduce the following partial substitution parameters for the C_{2v} ground-state structure: r_S(C—H) = 109.9 and r_S(C=Si) = 170.6 pm, and ∠H—C—H = 114.4°.

Than Si_2H_2 and $SiCH_2$ we could have no better demonstration of how remote open-shell reactive intermediates may be in their molecular and electronic structures from the familiar world of long-lived, closed-shell molecules with their apparent obedience to conventional bonding principles. Chemical studies of plasmas are still only in their infancy, and more new and exotic intermediates will surely come to light. Whatever we may make of their structures and bonding, they will have to be accommodated by any mechanistic proposal that seeks realistically to account for the reactions taking place in the discharge (*47*).

> Then felt I like some watcher of the skies
> When a new planet swims into his ken . . .

C. Trapping and Matrix Isolation

One way of catching and identifying a reactive transient is to intercept it with a reactive substrate so as to produce a known product that has a distinctive spectroscopic signature. For example, hydrogen atoms formed in the course of a reaction may be effectively scavenged by carbon monoxide to form the well-authenticated radical HCO, which can be identified unambiguously under appropriate conditions by its infrared or ESR spectrum (*48*). In a similar vein, ground-state sulfur atoms may be scavenged by dioxygen and detected indirectly by the infrared absorption or UV emission spectrum of the SO_2 molecules thus generated; by contrast, sulfur atoms in the excited ^1D state insert characteristically into the C–H bonds of alkanes (*48*). Some of the first evidence pointing to the formation of the trihydrides of aluminium and gallium came similarly from trapping experiments, this time with trimethylamine to form the known, relatively stable adducts $(Me_3N)_nMH_3$ (M = Al or Ga; n = 1 or 2) (*49*). With molecules as with atoms, it may be possible on the basis of suitable trapping

experiments to determine whether the intermediate is formed in its electronic ground state or in an excited state. "Singlet" dioxygen, that is, the O_2 molecule in its excited $^1\Delta_g$ electronic state, results from the stoichiometric oxidation of hydrogen peroxide by hypochlorous acid:

$$HOOH + HOCl \rightarrow {}^1O_2 + H_2O + HCl. \qquad (10)$$

It has a lifetime of only 2 μs in aqueous solution, but it may be intercepted and thereby distinguished from ground-state dioxygen by its facile addition to a conjugated molecule such as butadiene (*50*):

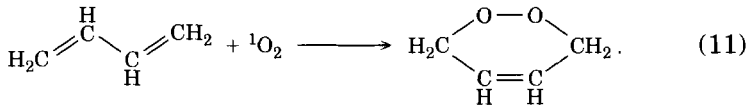

(11)

An alternative and more direct strategy involves matrix isolation (*51–53*). Here the trick is to catch and hold the intermediate by embedding it in a rigid, inert host such as solid argon (the matrix) at low temperatures (4–50 K). Hence, our fugitive is at once isolated and effectively immobilized. To some extent the experiments imitate nature, for the mineral lapis lazuli owes its beautiful blue color to the highly reactive radical anion S_3^-, which is entrapped in an aluminosilicate matrix. They also improve upon nature with the choice of a transparent, weakly interacting host such as a frozen noble gas at low temperatures, in place of the polar aluminosilicate, which is opaque to broad regions of electromagnetic radiation.

However short-lived the transient may be under normal conditions, its lifetime can be extended almost indefinitely by matrix isolation, and we can appeal to a variety of spectroscopic techniques—notably vibrational, electronic, and ESR methods—to follow what is going on in the matrix and to detect, identify, and characterize the trapped species. The method has great advantages. Spectroscopic measurements can be made at leisure and therefore in detail, and several different methods can be applied to interrogate a particular sample. Moreover, the infrared spectrum, which has been the principal agent of detection and analysis of matrix samples, is usually comparatively simple, with sharp linelike features marking the different transitions (and reflecting the conditions of low temperature, relatively isotropic, weakly interacting environment, and inhibition of rotation). Not only can vibrational frequencies meaningfully be measured to ± 0.1 cm^{-1}

in many cases, giving values close to those of the gaseous molecule, but the linelike character of the bands bids fair to the study of isotopic effects, frequently the most compelling means of determining the stoichiometry and geometry of the trapped molecule. On the other hand, there is also a price to be paid. Thus, inhibition of rotation means that we lose precise information about the dimensions, vibration/rotation, distortion, and charge distribution of the isolated molecule. In addition, various complications can arise from the weak but significant perturbations imposed on the trapped species by the cage it inhabits, which is likely to vary in size, geometry, and composition within a given matrix; as a result, specific spectroscopic transitions do not always appear as sharp bands but sometimes as multiplets or relatively broad bands. The combination of rapid quenching with the rigidity of the resulting condensate is also liable to lead to the trapping of different conformers of a particular molecule.

In practice no less than principle, the performance of a typical matrix-isolation experiment is quite simple. As illustrated in Fig. 8, a gas mixture is deposited under controlled, high-vacuum conditions on a cold surface the nature of which is dictated by the type of spectroscopic measurement to be made on the sample (*51–53*). The species of interest may be formed in the gas phase (by pyrolysis or in a discharge) and then quenched rapidly with an excess of the matrix gas; sometimes it is formed *during* the cocondensation of two reagents; commonly it is generated *in situ*, usually by irradiation of an appropriate matrix-isolated precursor.

As noted previously, identification of a novel or unfamiliar captive molecule is accomplished more often than not by reference to its infrared spectrum, with the following steps being typical of the way in which the experiment might proceed.

1. First, the number of distinct species present in the matrix has to be established; this is done by allocating the infrared absorptions to the appropriate species on the evidence of how the spectrum varies with changes in the experimental conditions.
2. We need then to assess the number, frequencies, and intensities of all the absorptions associated with a given molecule before drawing on the evidence of distinctive features due to specific groups, analogies with known compounds, or the vibrational selection rules in order to formulate its likely identity.
3. Evidence of identity is greatly strengthened if it is possible to devise an alternative route to the molecule in question starting from a different precursor. This strategy is well illustrated by the 16-electron

(a)

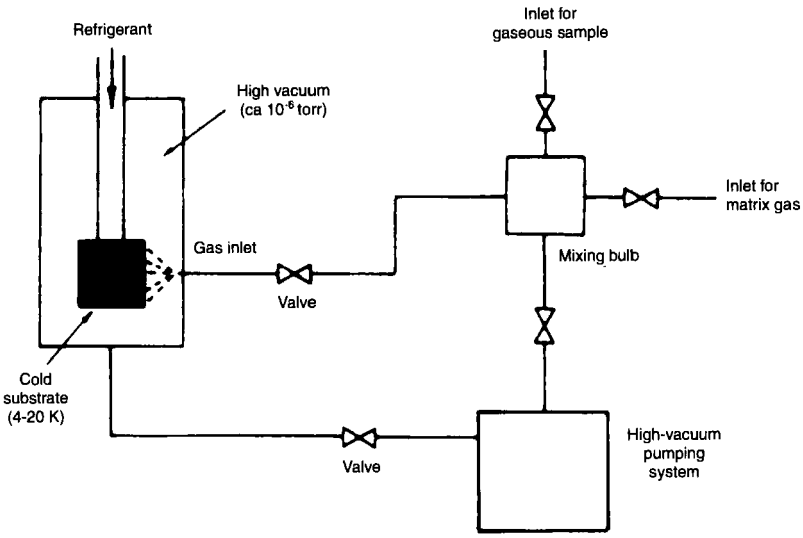
Refrigerant
Inlet for gaseous sample
High vacuum (ca 10^{-6} torr)
Inlet for matrix gas
Gas inlet
Mixing bulb
Valve
Cold substrate (4-20 K)
Valve
High-vacuum pumping system

(b)

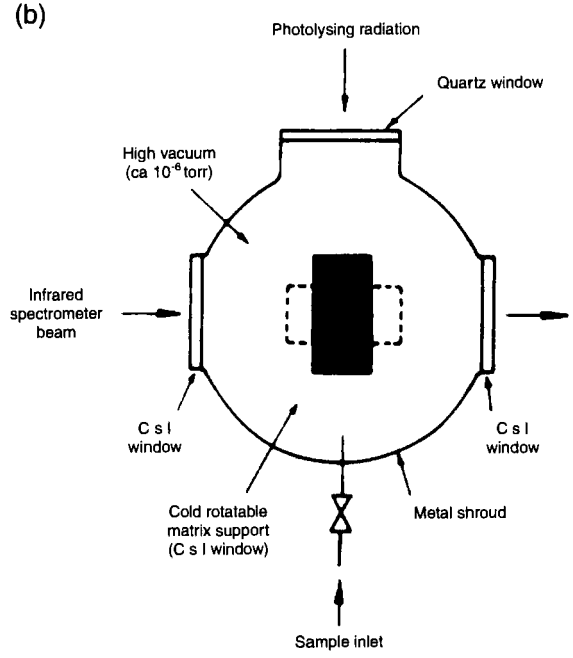
Photolysing radiation
Quartz window
High vacuum (ca 10^{-6} torr)
Infrared spectrometer beam
C s I window
C s I window
Cold rotatable matrix support (C s I window)
Metal shroud
Sample inlet

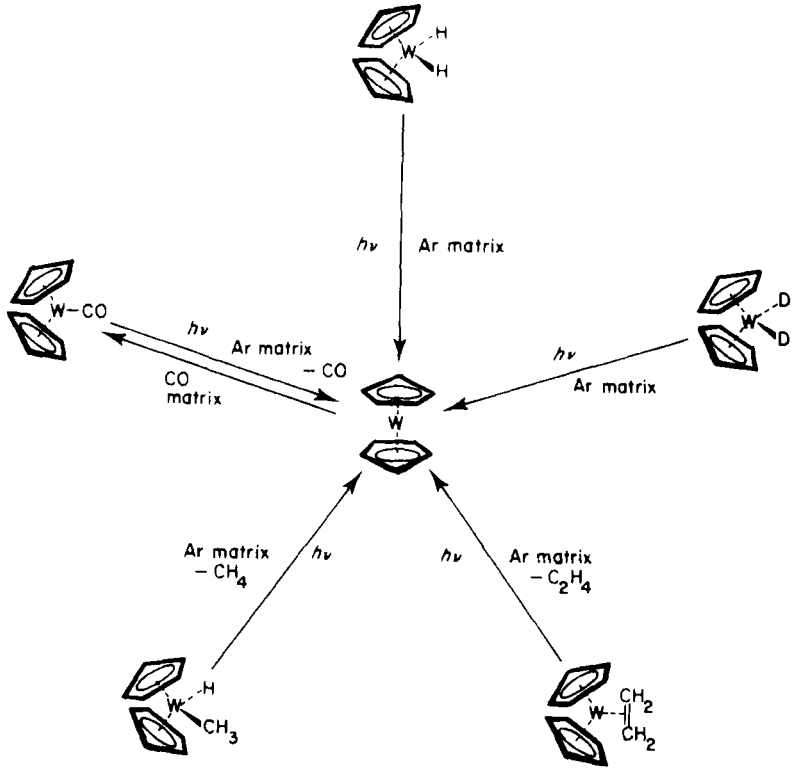

FIG. 9. Different routes leading to the unsaturated intermediate tungstenocene, $(\eta^5\text{-}C_5H_5)_2W$ [reproduced with permission from Downs, A. J.; Hawkins, M. *Adv. Infrared and Raman Spectrosc.* **1983,** *10,* 6].

intermediate "tungstenocene," $(\eta^5\text{-}C_5H_5)_2W$ (*54*), which has been shown by its infrared spectrum to be the common product of the matrix reactions set out in Fig. 9.

4. Annealing or photolysis of the matrix may also be instructive for the evidence of reactions such as (*55*)

$$2BH_3 \xrightarrow[27\ K]{\text{Ar matrix}} B_2H_6. \qquad (12)$$

FIG. 8. (a) Schematic representation of a typical matrix-isolation assembly. (b) Schematic plan of a matrix-isolation assembly suitable for infrared (transmission) measurements and for photolysis experiments [reproduced with permission from Almond, M. J.; Downs, A. J. *Adv. Spectrosc.* **1989,** *17,* 3].

5. Most revealing of all is usually the response of the spectrum to changes in the isotopic composition of the molecule. If the sample is prepared in such a way as to produce a mixture of isotopomers, then it is often possible to deduce unequivocally the stoichiometry and geometry of the molecule from the number, frequencies, and relative intensities of the infrared absorptions. With sufficient information, we may even be in a position to estimate one or more interbond angles, if these are not already fixed by the symmetry of the molecule. In the case of metal carbonyls, the vibrational problem can be simplified by concentrating on the restricted region of the infrared spectrum near 2000 cm^{-1}, corresponding to C–O stretching vibrations, ν(C–O), which can be successfully analyzed independently of the other fundamental vibrations through the use of an energy-factored force field. For each of several possible models of a particular metal carbonyl fragment $M(CO)_n$, it is then comparatively easy to estimate the frequencies and relative intensities of the ν(C–O) infrared bands for the family of isotopomers $M(^{12}CO)_x(^{13}CO)_{n-x}$ ($x = 0$–n) and so determine which model gives the best account of the observed spectrum. Figure 10 shows the results of applying this procedure (i) to $Fe(CO)_4$, the primary product of ultraviolet photolysis of $Fe(CO)_5$ (*56*), and (ii) to $O_2Mo(CO)_4$, a prominent intermediate in the train of reactions induced by ultraviolet photolysis of $Mo(CO)_6$ in the presence of O_2 (*57*). Hence, there is little doubt that $Fe(CO)_4$ has the C_{2v} structure **V** or that $O_2Mo(CO)_4$ has the *trans* configuration **VI** with a square planar $Mo(CO)_4$ fragment.

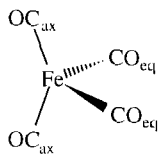

V

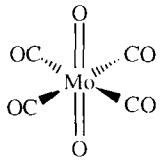

VI

6. The greatly enhanced sophistication of modern quantum chemical calculations means that we are now able to predict with considerable confidence the equilibrium structure of a molecule, the harmonic frequencies of its normal modes, and the intensities of the relevant features in infrared absorption. Accordingly, it has become quite commonplace with matrix as with other studies to test the inferences drawn from experiments against the results of appropriate *ab initio* or DFT analyses. How closely theory matches experiment is shown

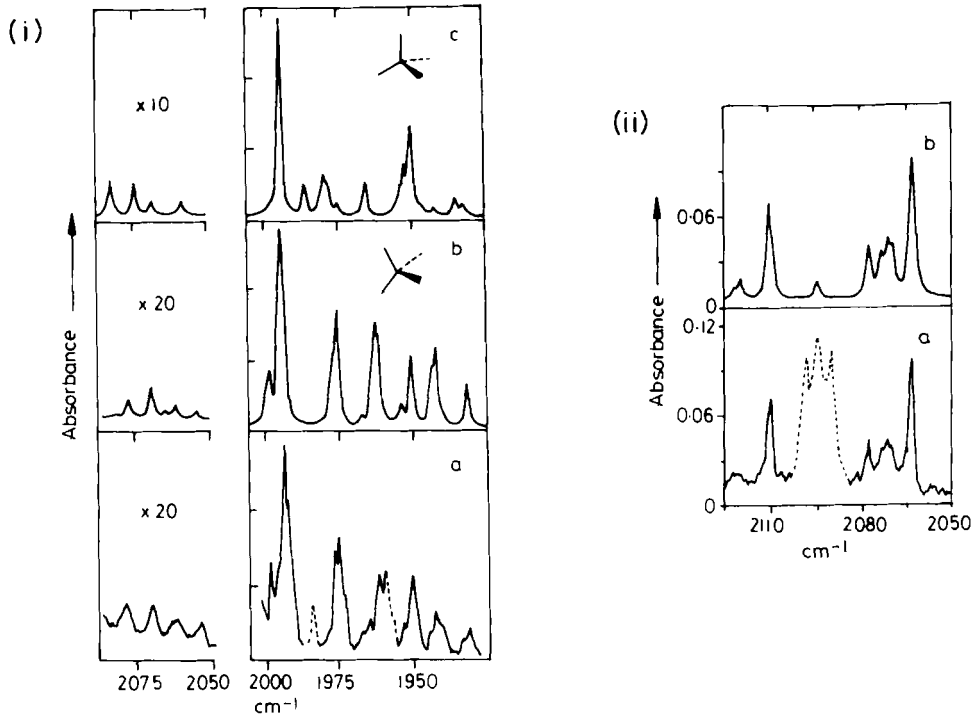

FIG. 10. (i) IR Spectra showing how the structure of matrix-isolated $Fe(CO)_4$ was established: (a) observed spectrum of $Fe(CO)_4$ with partial ^{13}CO enrichment isolated in a solid SF_6 matrix at 20 K [bands shown in dotted lines are due to residual $Fe(CO)_5$ precursor]; (b) spectrum calculated for the C_{2v} geometry, **V**, which gives the best agreement with the observed spectrum; (c) spectrum calculated for a C_{3v} geometry which provides a poor match to the observed spectrum (*56*). (ii) IR Spectra showing how the structure of *trans*-$O_2Mo(CO)_4$ was established: (a) observed spectrum of *trans*-$O_2Mo(CO)_4$ with partial ^{13}CO enrichment isolated in a solid CH_4 matrix (bands shown in dotted lines are due to photoejected ^{13}CO); (b) spectrum calculated for a planar $Mo(CO)_4$ fragment with D_{4h} symmetry, **VI** (*57*).

for the case of matrix-isolated Me_2AlNH_2 formed *in situ* by the elimination of CH_4 from the adduct $Me_3Al \cdot NH_3$ through irradiation with light at wavelengths near 210 nm (see Fig. 11) (*58*).

In relation to mechanistic enquiries, the principal strength of matrix isolation lies in the identification and specification of real or potential reaction intermediates. From such studies has come, for example, our first sighting of unsaturated molecules such as $Fe(CO)_4$ (*56*), $Fe_2(CO)_8$ (*59*), $Cr(CO)_5$ (*60*), $(\eta^5\text{-}C_5H_5)_2W$ (*54*), and $Ru(dmpe)_2$ (dmpe = $Me_2PCH_2CH_2PMe_2$) (*61*). The equilibrium structures of the ground-

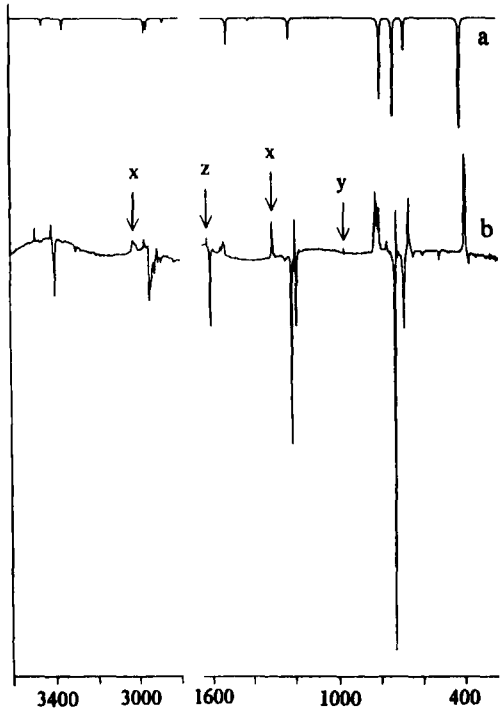

FIG. 11. IR Evidence for the formation of Me_2AlNH_2 by UV irradiation (λ = 210 nm) of the complex $Me_3Al \cdot NH_3$: (a) spectrum calculated for Me_2AlNH_2 at the RMP2(fc)/6-31G* level of theory; (b) difference IR spectrum after irradiation of $Me_3Al \cdot NH_3$ (decreasing absorptions point downward; increasing absorptions point upward). **x** indicates CH_4, **y** indicates NH_3, and **z** indicates H_2O (impurity) [reproduced with permission from (*58*), p. 6372].

state molecules appear to be independent of the matrix material (provided that there is no direct reaction with the matrix), and the case histories of numerous molecules affirm that the same structures persist in the fluid phases. About the electronic and photochemical properties of such molecules there is much also to be gleaned through matrix isolation, so there can be little doubt, for example, that $Fe(CO)_4$ has a triplet electronic ground state or that $Cr(CO)_5$ as initially generated by photolysis of $Cr(CO)_6$ is in a vibrationally or possibly electronically excited state. Some clear sign of the reactivity of the molecule may be found. In this regard, few experiments are more striking or more significant than those in which the visible absorption spectrum of $Cr(CO)_5$ is found to vary dramatically according to the nature of the matrix in which the molecule is trapped (*60*). Hence we

learn just what an extraordinarily powerful Lewis acid $Cr(CO)_5$ is, for the unsaturated molecule, which has a square pyramidal (C_{4v}) structure, evidently interacts to an appreciable extent through the vacant, sixth coordination site even with a matrix molecule such as CH_4, Xe, or Ar that has few claims to be regarded as a normal ligand. Experiments with mixed matrices have shown that the token ligand is interchanged by irradiating selectively into the characteristic electronic absorption band at lowest energy. Because the molecules are not free to rotate, it is possible to select those in certain orientations by the use of plane-polarized photolyzing radiation and so generate products in orientations that can be analyzed spectroscopically, also with the aid of polarized light. Hence, the interchange reactions are found to occur by expulsion of one token ligand, followed by a Berry pseudorotation, and uptake of another token ligand (Fig. 12). There is still much that we do not know about $Cr(CO)_5$ and its photochemistry, but these matrix studies have surely opened our eyes to the nature of this particular intermediate and the part it plays in the supposedly simple substitution reactions of $Cr(CO)_6$.

However, matrix studies are limited ultimately by the low mobility of the caged species, allied to the narrow temperature range over which they can be held. The very immobilization that helps to preserve a highly labile molecule in a solid matrix becomes an Achilles' heel when we wish to explore its reactions. The restraining effect of the matrix cage is much in evidence in the way photodissociation or photoisomerization reactions are immediately arrested and in the way bimolecular reactions induced by photolysis are normally restricted to neighboring pairs of molecules. Reaction channels that are important in the mobile fluid phases may thus be debarred, whereas other channels of minor importance in the fluid phases may well be favored. For example, photolysis of the recently identified chlorine oxide $ClClO_2$ (formally a dimer of ClO) results in isomerization to ClOClO and ClOOCl when the molecules are confined to a matrix, but yields Cl_2 and O_2 as the only detectable products in the gas phase (*62*). We have already considered the scope that exists for recognizing and characterizing reactive intermediates in the gas phase. What options are there for extending our investigations to the liquid phase and to solutions?

D. Solution Studies at Low Temperatures

Various problems are inherent in the solution state when it comes to tracking reactive intermediates. First, the solvent may be a far

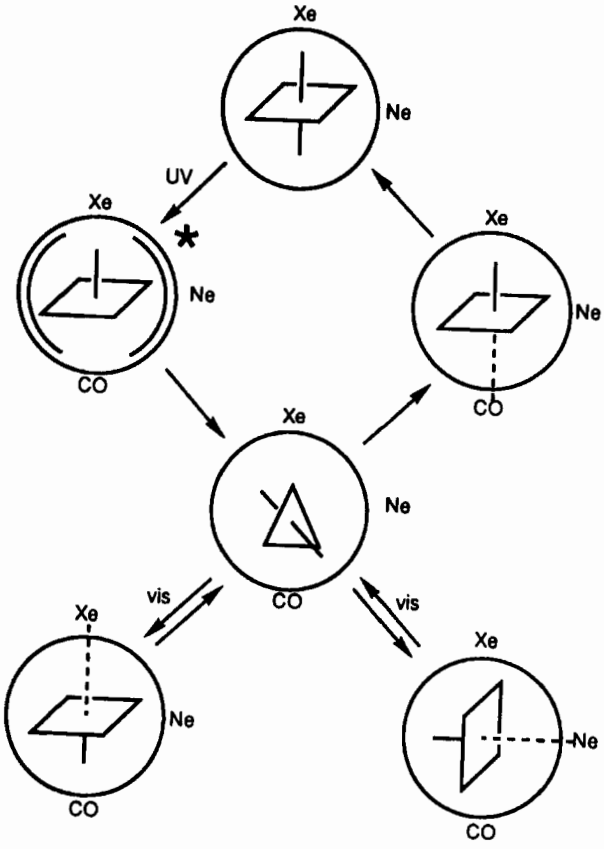

FIG. 12. Schematic representation of the photochemical behavior of the $Cr(CO)_5$ fragment in a mixed Ne/Xe matrix at low temperatures. * represents the C_{4v} fragment in the excited ^1E state [reproduced with permission from (*60*), p. 136].

from innocent spectator; second, as with matrix samples, rotational transitions are not a feasible source of information; third, the spectroscopic features due to a solute molecule are appreciably broader than those of the same molecule in a solid, inert matrix, so that isotopic effects are much harder to evaluate; and last, most solvents absorb strongly in many regions of the electromagnetic spectrum, thereby obscuring our vision of the solute species in these regions. Nevertheless, the simple expedient of cooling a solution may be sufficient to extend the lifetime of an intermediate to the point at which it can be detected by conventional spectroscopic means. A good example is the vinyl hydride complex $(\eta^5\text{-}C_5H_5)Ir(\eta^1\text{-}C_2H_3)(\eta^2\text{-}C_2H_4)H$ (**VII**). This is

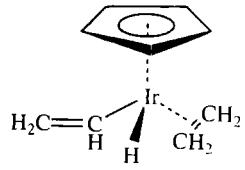

VII

one of the intermediates formed by photolysis of the corresponding bis(ethene) complex $(\eta^5\text{-}C_5H_5)Ir(\eta^2\text{-}C_2H_4)_2$ with light having wavelengths >290 nm (*63*). The photoinsertion into a C–H bond of a coordinated ethene molecule can be engineered simply by photolyzing a frozen [$^2H_8$]toluene glass at 77 K, and the vinyl hydride can be recognized definitively by thawing the glass and measuring the ^1H and ^{13}C NMR spectra of the resulting solution at *ca.* 230 K; raising the temperature to 273 K results in slow decomposition, with reversion to the starting material.

There is much to be gained from the use of a very weakly coordinating solvent such as a liquefied or even supercritical noble gas (*64*, *65*). The noble gases may each have a very narrow liquid range at low pressure, but by working at pressures of 20 bars or more it is possible to span the entire range from 77 K to ambient temperatures with liquid argon, krypton, and xenon. Ill adapted though these liquids may be for the dissolution of polar compounds, they are capable of dissolving more or less freely many organic and organometallic materials as well as gases such as H_2, N_2, CO, and CH_4, and analysis of the resulting solutions is hugely facilitated by the absence of solvent absorption in the infrared, visible, and normal ultraviolet regions, with the result that much longer pathlengths are admissible than for conventional solution studies. Accordingly, we can draw on a range of conventional spectroscopic methods to examine the solutions. Bandwidths may be appreciably greater than for matrix spectra, but problems of matrix site effects are eliminated and the bands are regular and symmetrical in shape. Moreover, the solutions give much flatter spectroscopic baselines than do matrices; allied to the advantage of the long pathlength, this increases considerably the capacity to detect weak bands. More fundamentally still, and in contrast with matrix studies, solution-based measurements provide the opportunity of exploring the kinetics and positions of equilibrium of reactions under thermal control. At the same time, we lose sight of some intermediates revealed by matrix isolation or other means that do not survive

in solution, at least long enough to be detected by normal means. Solution experiments may thus succeed in recording the fate of a labile, coordinatively saturated organometallic molecule such as $Cr(CO)_5(N_2)$ but not of a coordinatively, unsaturated one such as $Cr(CO)_5$.

Figure 13 shows the design of one such cell as used by Poliakoff and Turner and their group at Nottingham for experiments of this sort (*64*). The cell is cooled by liquid nitrogen, the flow of which is pulsed to vary the temperature. An important feature not illustrated in the figure is the presence within the cell of a microscale magnetic stirrer "flea"; hence, even solutions that are strongly absorbing in the ultraviolet or visible regions can be made to react photochemically because the portion of solution immediately adjacent to the irradiation window is constantly being renewed. For photochemically generated compounds that have lifetimes in the order of seconds, it may be

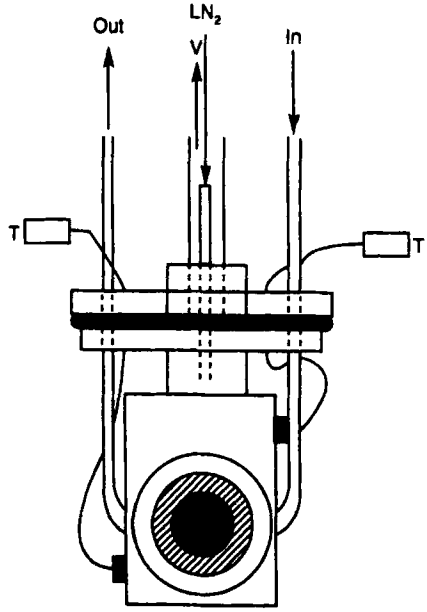

FIG. 13. Schematic view of a variable temperature cold cell used for infrared studies of liquid noble-gas solutions. Cooling is achieved with a pulsed flow of liquid N_2 (LN_2) controlled by the output from one of the two thermocouples T so as to stabilize the temperature. The whole cell fits into a vacuum jacket (not illustrated), which is pumped through the tube V in the top flange of the cell. The solution under study can be passed through the cell from a room temperature reservoir via the two tubes marked In and Out [reproduced with permission from (*81*), p. 555].

necessary to record the spectrum *while* the solution is being irradiated.

Some idea of the compass of such studies may be gained from the case of the dihydrogen complex $Cr(CO)_5(\eta^2\text{-}H_2)$, which for all its 18-electron configuration, is too labile to be isolated or spotted by ordinary methods of attack. The complex can be detected following photolysis of $Cr(CO)_6$ or $Cr(CO)_5(NH_3)$ in an H_2-doped matrix, but the matrix testimony has to rely principally on ν(C–O) bands in the infrared spectrum; the broad ν(H–H) feature near 3000 cm^{-1} is some 20 to 30 times weaker than the least intense of the ν(C–O) bands and, not surprisingly, is barely visible above irregularities in the baseline. These findings have been largely eclipsed, though, by the results of experiments involving photolysis of $Cr(CO)_6$ dissolved in liquid xenon under a pressure of H_2. Using these conditions, the Nottingham group has succeeded in detecting a weak, broad infrared absorption fulfilling all the requirements for assignment to the ν(H–H) mode of the coordinated H_2 moiety (*66*). The absorption comes at 3030 cm^{-1} when H_2 is the ligand, shifting to 2241 cm^{-1} when H_2 gives way to D_2. On the other hand, similar experiments starting from the bis(ethene) complex $(\eta^5\text{-}C_5H_5)Rh(\eta^2\text{-}C_2H_4)_2$ reveal the formation not of a dihydrogen complex but of the unstable dihydrido derivative $(\eta^5\text{-}C_5H_5)Rh(\eta^2\text{-}C_2H_4)(H)_2$ (*67*).

Ultraviolet irradiation of a liquid xenon solution of $Cr(CO)_6$ without any other agent generates a new species that, with a half-life of about 2 s at 175 K, is sufficiently long-lived to be detected by conventional infrared measurements. The species has ν(C–O) absorptions very close in frequency and intensity pattern to those assigned to the matrix-isolated species $Cr(CO)_5$···Xe (*64*). Its identity can be checked, first by deliberately doping the solution with a range of likely impurities in order to rule out the possibility of its being some other compound of the type $Cr(CO)_5L$ (L = N_2, H_2O, etc.), and second, by carrying out experiments with $Cr(CO)_6$ dissolved in pure liquid krypton and in liquid krypton doped with 5% xenon. Hence, the realization is dawning that the coordination of $Cr(CO)_5$ by xenon involves not a generalized solvation but a specific interaction with the formation of a Cr–Xe bond of appreciable strength.

Similarly, the transient $Ni(CO)_3(N_2)$ has been identified following its generation by photolysis of $Ni(CO)_4$ in liquid krypton doped with N_2 at 114 K. Ultraviolet irradiation establishes a steady-state concentration of $Ni(CO)_3(N_2)$; as soon as the photolysis source is switched off, the dinitrogen complex begins to decay, reacting thermally with CO to regenerate $Ni(CO)_4$. The kinetics of the decay reaction,

$$Ni(CO)_3(N_2) + CO \rightarrow Ni(CO)_4 + N_2, \quad (13)$$

have been investigated in some detail over the temperature range 112–127 K (*68*). The rate shows a first-order dependence on the concentration of $Ni(CO)_3(N_2)$ and a more complex dependence on the concentrations of CO and N_2. Hence, it appears that the reaction proceeds via two simultaneous paths, one dissociative and the other probably associative. An estimate of about 42 ± 4 kJ · mol^{-1} for $\Delta H\ddagger$ for the dissociative path gives a measure of the Ni–N_2 bond dissociation enthalpy in $Ni(CO)_3(N_2)$.

In an extension of the technique we can now trade on the remarkable properties of supercritical fluids (*64*, *69*). These combine a number of properties of gases and liquids; like gases they are highly compressible and are completely miscible with H_2 or N_2, but like liquids they are relatively dense and dissolve a wide range of nonionic solids. In fact, most materials are considerably more soluble in supercritical xenon than in liquid xenon, despite the fact that the density of the supercritical material at the critical point is only about one-third that of liquid xenon. Moreover, the solubility of any compound in a supercritical fluid increases with increasing pressure at a constant temperature, with the result that the solvating power of the medium can be tuned by varying the pressure. It is the superior solubility of compounds that gives supercritical solvents a major advantage over their normal liquid counterparts and particularly in reactions involving gases such as H_2 or N_2. Thus, for a given pressure of gas, the effective concentrations of H_2 in a supercritical solution can be nearly an order of magnitude higher than in a liquid solution. As a result, it is altogether easier to detect, preserve, and even synthesize known or potential reaction intermediates. Previously unknown dihydrogen and dinitrogen complexes, which would normally decay rapidly at ambient temperatures, have thus been formed in supercritical xenon, where they are sufficiently robust at room temperature to be characterized quite normally by their infrared spectra (*69*, *70*). Kinetic measurements between 283 and 353 K show that (η^6-C_6H_5Me)$Cr(CO)_2$(η^2-H_2) reacts with CO in accordance with Eq. (14), with an activation enthalpy of 70 ± 5 kJ · mol^{-1}, which may correspond to the Cr–H_2 bond dissociation enthalpy:

$$(\eta^6\text{-}C_6H_5Me)Cr(CO)_2(\eta^2\text{-}H_2) + CO \rightarrow (\eta^6\text{-}C_6H_5Me)Cr(CO)_3 + H_2. \quad (14)$$

This conclusion finds support from more recent studies, also at high pressure but in *n*-heptane solution and using photoacoustic calorime-

try to measure the enthalpy change of Reaction (15) (*71*),

$$M(CO)_6 + L \rightarrow M(CO)_5L + CO \qquad (15)$$

(M = Cr or Mo; L = *n*-heptane, H_2 or N_2);

the Cr–H_2 and Cr–N_2 bond enthalpies are estimated in this case to be 78 and 81 kJ · mol^{-1}, respectively.

Figure 14 illustrates the region of the infrared spectrum associated with ν(N–N) modes for a supercritical xenon solution of the rhenium carbonyl (η^5-C_5H_5)Re(CO)$_3$ under a pressure of N_2 (*ca.* 90 bars) and shows how this changes with time on photolysis with ultraviolet light (*70*). The spectrum bears clear witness to the sequential formation of the species (η^5-C_5H_5)Re(CO)$_2$(N_2), (η^5-C_5H_5)Re(CO)(N_2)$_2$, and (η^5-C_5H_5)-Re(N_2)$_3$ at room temperature, and the last two turn out to be surprisingly stable under these conditions. In suitable circumstances, solutions in supercritical solvents are amenable even to NMR measurements (*72*). Supercritical fluids are thus affording a new dimension and are giving direct access to new chemistry involving reactive intermediates, as well as a new approach to problems of analysis, synthesis, and materials processing.

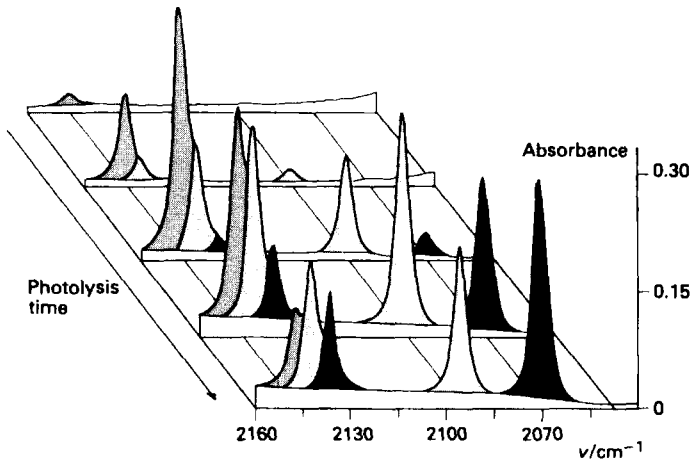

FIG. 14. IR spectra showing the sequential formation of (η^5-C_5H_5)Re(CO)$_2$(N_2) (dark peaks), (η^5-C_5H_5)Re(CO)(N_2)$_2$ (medium peaks), and (η^5-C_5H_5)Re(N_2)$_3$ (light peaks) from (η^5-C_5H_5)Re(CO)$_3$ and N_2 in supercritical xenon solution [reproduced with permission from Poliakoff, M.; Howdle, S. *Chem. Br.* **1995,** *31,* 120].

IV. Experimental Characterization of Reaction Intermediates: Time-Resolved Methods

To retard or suppress chemical reactions it has been necessary to work under rather unusual conditions. It is only natural to want to know about the behavior of intermediates under more normal conditions. However, if the species are highly reactive, detection and monitoring of their fate demand very rapid spectroscopic measurements. From the more or less conventional type of spectroscopic analysis that has been the mainstay of our investigation so far we pass to methods that can be adapted to real-time measurements and in which spectral evolution or decay can be monitored at intervals sometimes as short as femtoseconds. It will soon be apparent, though, that the knowledge about the kinetic correlation between intermediates, reagents, and products thus gained can only be at the expense of detailed knowledge about the physical properties of the molecules—sometimes even their very identities. The function of the gas-phase, supersonic-jet, matrix-isolation, and low-temperature solution techniques described in the preceding sections is in the provision of a "spectral library" of more or less well-authenticated reaction intermediates, whether real or model ones; this library is going to prove essential to the interpretation of many time-resolved experiments.

The most popular procedure involves *flash photolysis* or, in the terms of laser technology, *pump-and-probe* experiments (*73–76*). Flash photolysis was developed by Norrish and Porter in Cambridge in the 1940s and earned them the Nobel Prize in 1967. The basis of the technique is simplicity itself. A pulse of light is used to generate the transient, typically in a fluid sample at or near ambient temperatures, and a spectroscopic record of the sample in absorption or emission is then kept *as a function of time.* The time-scales of the reactions that can be studied are limited by the duration of the initiating light pulse. The flash lamps used by Norrish and Porter, which give pulse durations of several milliseconds, have now been largely superseded by high-powered lasers giving pulse durations of nanoseconds or less. By means of a process called mode-locking it is possible even to generate laser pulses lasting only a few picoseconds or less; the world record is currently reported to be 4 femtoseconds. Such lasers offer a means of tracking very fast kinetic phenomena, such as the isomerization of an electronically excited alkene, the rotational motion of a large molecule in solution, or some of the fast processes occurring in photosynthesis. Although these ultrafast processes (*77*) are not "reactions" in the sense that we have discussed so far, they are none-

theless important in the contributions they may make to overall reactions.

An alternative technique for the rapid generation of transient species is that of pulse radiolysis triggered not by a light flash but by a short pulse (10^{-9}–10^{-6} s) of high-energy electrons (1–5 MeV); this approach has been employed primarily for studies of liquid phase kinetics and especially of the solvated electron, but it is a very flexible method with applications also for gas phase studies (*78*). Representative of this method of attack is the formation of the peroxynitrate anion O_2NOO^- less than 2 ms after pulse irradiation of aerated aqueous solutions containing nitrate and formate at relatively low concentrations (*79*). The anion, which can be detected and monitored by its UV absorption near 290 nm, is a strong oxidizing agent notable for its potential mediation in some of the reactions that make living systems vulnerable to nitrogen dioxide, one of the most toxic components of polluted atmospheres. It is of some consequence therefore that studies of several oxidation reactions should reveal two distinct pathways by which the peroxynitrate decays, one proceeding through the parent acid O_2NOOH and the other probably evolving through secondary reactive intermediates derived from the decomposition of the peroxynitrate.

Once the transient species has been formed, it has to be monitored by some form of kinetic spectroscopy, typically with ultraviolet-visible absorption or emission, infrared (time-resolved infrared or TRIR) (*74*), or resonance Raman (time-resolved resonance Raman or TR^3) (*80*) methods of detection. The transient is usually tracked by a probe beam at a single characteristic frequency, thereby giving direct access to the kinetic dimension. Spectra can then be built up point by point, if necessary, with an appropriate change of probe frequency for each point, although improvements in the sensitivity of multichannel detectors may be expected to lead increasingly to the replacement of the laborious point-by-point method by full two-dimensional methods of spectroscopic assay (that is, with both spectral and kinetic dimensions).

Ultraviolet-visible absorption has traditionally been the basis of detection in flash photolysis experiments. It offers a number of advantages in sensitivity and efficiency and has certainly delivered much vital information about the reactivity of transient species. On the other hand, the ultraviolet-visible absorption bands characteristic of any but the simplest molecules tend to be broad and relatively uninformative as regards identity and structure, and so we may run into problems not only with the overlap of absorptions due to different

species, but also with deciding on the nature of the carrier of a particular absorption spectrum. Altogether more discriminating, albeit less sensitive, are the TRIR methods that have been successfully developed in the past 15 years or so (*74*, *81*). With the sort of apparatus depicted schematically in Fig. 15, it has been possible to draw on the spectral library built up from matrix isolation and other experiments in the "slow" regime to identify transients formed in the gas phase or in solution at ambient temperatures, as well as investigating their kinetic behavior. Just what can be achieved in this way will be demonstrated by some examples representative of recent studies.

As a start, we return to that remarkable Lewis acid $Cr(CO)_5$. Flash photolysis experiments have been carried out with $Cr(CO)_6$ either in solution or in the gas phase and with either infrared or visible probes (*9*, *60*). For example, photolysis of gaseous $Cr(CO)_6$ with the output of an XeF laser yields a predominant transient that can be tracked by a

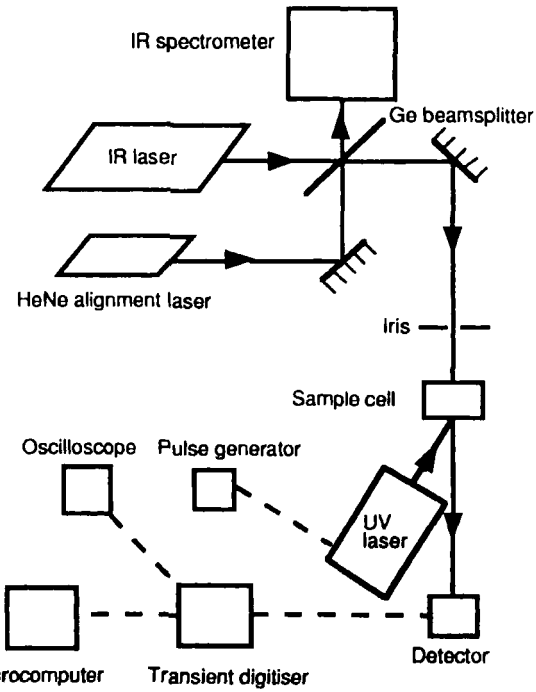

FIG. 15. Schematic representation of the time-resolved infrared (TRIR) flash photolysis apparatus used at Nottingham. The UV pulse laser generates transient species; the continuous IR laser monitors the change in transmission at a particular IR frequency, producing a trace showing the IR absorbance as a function of time. The experiment is repeated at different IR frequencies so that a complete IR spectrum of the transient can be built up [reproduced with permission from (*97*), p. 103].

line-tunable, liquid-nitrogen-cooled CO laser, changes in intensity of the transmitted infrared light being recorded by a high-speed InSb detector. The ν(C–O) bands clearly imply that the species is "naked" $Cr(CO)_5$ (freed at last from any token ligand) with the same square pyramidal geometry as the molecule identified previously by matrix isolation (see Section III,C). The identification is confirmed by the decay of the transient at a rate matching the rate of reappearance of $Cr(CO)_6$. The rate constant for the reaction of $Cr(CO)_5$ with CO at 293 K comes out to be $1.5 \pm 0.3 \times 10^{10}$ $dm^3 \cdot mol^{-1} \cdot s^{-1}$. Similar studies of the reaction of $Fe(CO)_4$ with CO give a rate constant about two orders of magnitude smaller (*56*). This difference can be rationalized, at least in part, with the realization that $Fe(CO)_4$ has a triplet ground state whereas $Cr(CO)_5$ almost certainly has a singlet ground state. Closer examination shows that $Cr(CO)_5$ is generated within 1 picosecond of light absorption and that it is formed in vibrationally excited states that relax over tens if not hundreds of picoseconds (*60*). These details emerge not only from time-resolved ultraviolet-visible studies but also from analogous TR^3 experiments with cyclohexane solutions in which two 5-ps pulses at $\lambda = 266$ nm are employed; the first dissociates $Cr(CO)_6$, and the second probes the resonance Raman spectrum of the photoproduct $Cr(CO)_5$. Hence, it appears that the naked intermediate, albeit vibrationally excited, can exist for a few picoseconds before taking up a solvent molecule.

Extension of these studies to supercritical fluids provides a way of making TRIR measurements on intermediates incorporating a bond between a metal center and a weakly coordinating ligand such as a noble gas or CO_2. Hence, for example, a series of organometallic noble-gas compounds, $W(CO)_5(Ar)$, $M(CO)_5(Kr)$, and $M(CO)_5(Xe)$ (M = Cr, Mo, or W), have been detected transiently in fluid solution at room temperature (*82*). The second-order rate constants for the reaction of $M(CO)_5L$ with CO show that the reactivity for a given metal M varies in the order L = Kr > Xe $\approx$ CO_2, whereas the reactivity for a given ligand L varies in the order M = Cr $\approx$ Mo > W. The reaction of $W(CO)_5(Xe)$ with CO has an enthalpy of activation of 34 $kJ \cdot mol^{-1}$, representing a lower limit for the W–Xe bond enthalpy. The bond is therefore twice as strong as a conventional hydrogen bond, and its mechanistic impact cannot be ignored.

The photochemistry of the binuclear iron carbonyl $[(\eta^5\text{-}C_5H_5)Fe(CO)_2]_2$, **VIII**, provides another outstanding example of the interplay between time-resolved and alternative strategies (*76*). According to the infrared spectrum of this compound in a suitable matrix at low temperatures (*83*), ultraviolet photolysis results in the elimination of free CO, but the pronounced cage effect of the medium entirely sup-

presses the separation of $(\eta^5\text{-}C_5H_5)Fe(CO)_2$ radicals, **X**. Experiments with a ^{13}CO-labeled sample demonstrate that the iron-containing product formed by CO loss has a binuclear framework incorporating three CO bridges, **IX**:

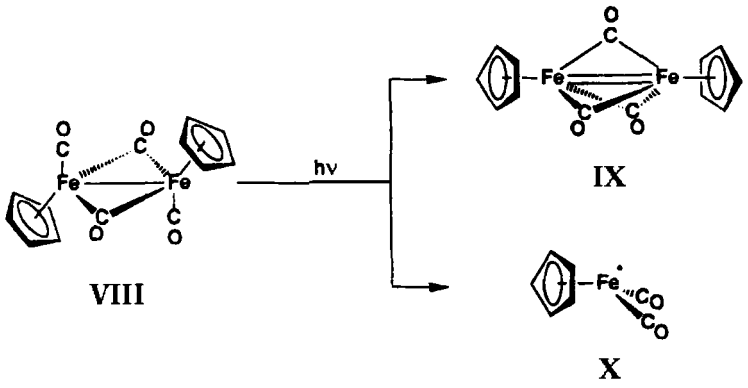

(16)

Pulsed laser photolysis (at λ = 308 nm) of **VIII** in an alkane solution at room temperature can be shown by TRIR measurements to generate not one but two metal carbonyl species with quite different kinetic properties (*84*). One transient displaying two infrared bands characteristic of the ν(C–O) modes of terminal CO groups decays rapidly by second-order kinetics (with $k_2 = 5 \times 10^9$ dm$^3 \cdot$ mol$^{-1} \cdot$ s^{-1}) to regenerate the precursor within about 50 μs. The infrared spectrum of this species, allied to its other properties, makes clear that it is the radical $(\eta^5\text{-}C_5H_5)Fe(CO)_2$, **X**. The second transient is the triply CO-bridged complex **IX**, easily recognizable by the close resemblance its infrared spectrum bears to that of the matrix-isolated species. In the absence of added CO, this has a half-life of about 0.6 s—that is, some four orders of magnitude longer than that of the radical. **IX** reacts with CO, and its decay as well as the regeneration of **VIII** can also be monitored by TRIR measurements. Similar experiments with another substrate L to form the product $(\eta^5\text{-}C_5H_5)_2Fe_2(CO)_3L$ [e.g., L = CH_3CN or $P(OMe)_3$, see Fig. 16] reveal the participation of both intermediates **IX** and **X** through parallel reaction paths. The reactivity of the radical **X** may thus be gauged by rate constants close to the diffusion-controlled limit. For another string to our spectroscopic bow we may also turn to Raman scattering, using a single visible laser to fulfil the dual functions of pump and probe, and detecting the emitted light by a suitable optical multichannel analyser. Cyclohexane solutions of $[(\eta^5\text{-}C_5H_5)Fe(CO)_2]_2$ and its permethylated analog $[(\eta^5\text{-}C_5Me_5)Fe(CO)_2]_2$ show resonance Raman behaviors correlating with the lower energy

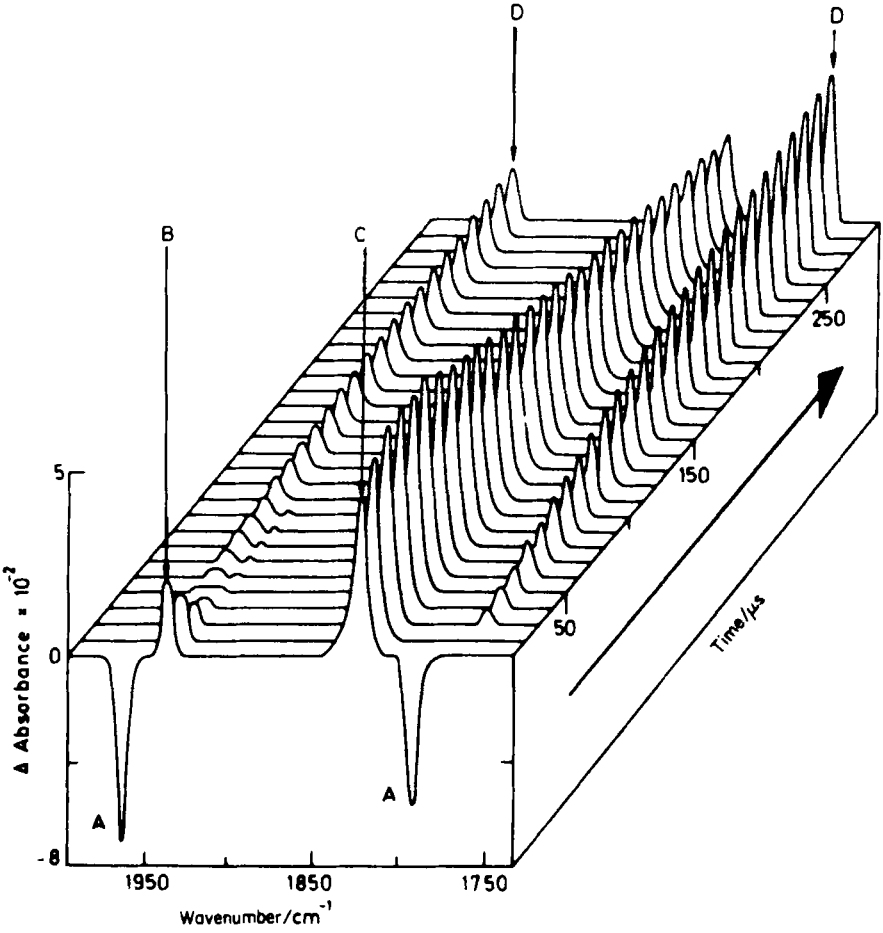

FIG. 16. Time-resolved infrared spectrum obtained after UV flash photolysis of $[(\eta^5\text{-}C_5H_5)Fe(CO)_2]_2$, **VIII** (A), and MeCN in cyclohexane solution at 25°C. The bands are labeled thus: B, $(\eta^5\text{-}C_5H_5)Fe(CO)_2$, **X**; C, $(\eta^5\text{-}C_5H_5)_2Fe_2(\mu\text{-}CO)_3$, **IX**; and D $(\eta^5\text{-}C_5H_5)_2Fe_2(CO)_3(MeCN)$. The first three spectra correspond to the duration of the firing of the UV flash lamp, and subsequent spectra are shown at intervals of 10 μs. The negative peaks in the first spectrum are due to material destroyed by the flash; these have been omitted from the subsequent traces to avoid undue confusion [reproduced with permission from Dixon, A. J.; Healy, M. A.; Poliakoff, M.; Turner, J. J. *J. Chem. Soc., Chem. Commun.* **1986,** 994].

electronic absorption bands, thereby shedding light on the molecular orbitals involved in the electronic transitions (*85*). By the simple device of increasing the incident laser power it is possible to observe additional rich resonance Raman spectra that must originate in the binuclear transients $(\eta^5\text{-}C_5R_5)_2Fe_2(\mu\text{-}CO)_3$, where R = H (**IX**) or Me.

With its different requirements, the Raman effect gives access to vibrational transitions that may well be lost to view in infrared absorption.

Time-resolved Raman spectroscopy, both spontaneous and coherent, has developed apace in the past two decades (*86*). As a means of pursuing short-lived intermediates, spontaneous resonance Raman scattering has proved particularly instructive, partly because of its high selectivity, partly because of its enhanced sensitivity. Since studies of this sort were initiated in 1976, the time resolution has improved from microseconds to subpicoseconds. The method has really come into its own, notably in the hands of Kitagawa and his colleagues at Okazaki (*87*), in the investigation of heme proteins and of how they bind dioxygen and other ligands. For example, the reaction of dioxygen with the reduced enzyme cytochrome *c* oxidase (CcO), formed by CO photodissociation in aqueous solution, has been followed by TR^3 measurements (*87*), which reveal within 10 ms the growth and decay of several intermediates identifiable by emissions due to O–O or Fe–O stretching vibrations in the region 300–850 cm^{-1}. The origins of the bands have been traced by experiments with ^{18}O-enriched samples of O_2, and hence it can be shown that the O_2 binds initially to the Fe_{a3} site in CcO in an end-on fashion with an Fe–O–O bond angle close to 120°. Studies with picosecond time resolution witness within 5 ps of photolysis of the CO-bound precursor an intermediate believed to be the high-spin, five-coordinate heme Fe^{2+}_{a3} to which a histidine (His) is ligated; this is indicated by the growth of a band at 220 cm^{-1} attributable to the Fe–His vibration (*88*).

Intense interest in how carbon–hydrogen bond activation may be engineered has led to detailed studies of several transition-metal compounds known to compass reactions of this type, which are sometimes initiated thermally, but more often photochemically. Two such compounds are the iron and ruthenium dihydrides $M(dmpe)_2H_2$ (M = Fe or Ru; dmpe = $Me_2PCH_2CH_2PMe_2$), which react with alkanes RH under irradiation in accordance with Eq. (17) (*61*, *76*):

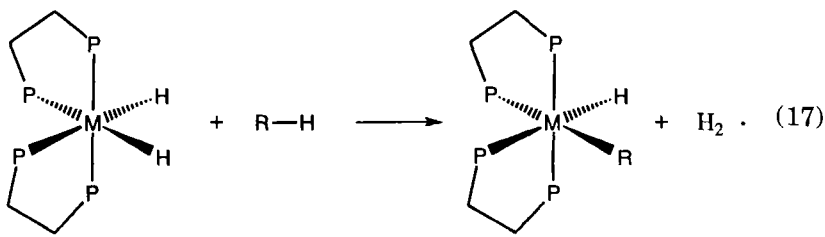

(17)

The ruthenium compound gives an object lesson in the merits of combining matrix with time-resolved solution studies. Photochemical reductive elimination of H_2 may be followed by the decay of the characteristic ν(Ru–H) bands in the infrared spectrum or by the growth of three intense visible bands at *ca.* 740, 540, and 460 nm. Although the product lacks characteristic infrared features, the circumstances of its formation and its response to matrix dopants imply that it is the 16-electron species $Ru(dmpe)_2$, presumably with a square planar skeleton.

Flash photolysis of a cyclohexane solution of the dihydride with a pulsed laser yields a transient with a visible spectrum remarkably like that of the matrix photoproduct. The transient signal decays by second-order kinetics over *ca.* 80 μs as the precursor is regenerated. Addition of H_2 even in very low concentration increases the rate of decay, causing it to become pseudo–first order; under these conditions the reaction of the intermediate with H_2 is essentially diffusion controlled, being opposed by a minimal activation barrier. The corresponding iron compound $Fe(dmpe)_2H_2$ cannot be vaporized without decomposition and so does not lend itself to matrix isolation, but flash photolysis of an alkane solution at room temperature gives a transient $Fe(dmpe)_2$ differing conspicuously from its ruthenium counterpart. For one thing, its electronic absorption spectrum shows but a single band at low energy, and that not in the visible but in the near-ultraviolet region. The reactivities are quite different too: both intermediates add substrates to form products of the type $M(dmpe)_2L$, where L = CO, C_2H_4, or PMe_3, as well as reacting with H_2, certain hydrocarbons, or Et_3SiH to give insertion products of the type $M(dmpe)_2(X)(H)$ (X = H, organic group, or Et_3Si), with the kinetic results summarized in Fig. 17. The reactions with H_2, Et_3SiH and alkenes are slower by at least two orders of magnitude for $Fe(dmpe)_2$ than for $Ru(dmpe)_2$, whereas alkanes and arenes find $Fe(dmpe)_2$ much the more reactive of the two. One plausible explanation of the spectral and kinetic differences is that the intermediates have different structures, with $Fe(dmpe)_2$ adopting a "butterfly" configuration unlike the square planar form of its ruthenium analog, although we lack definitive evidence on this point. The reduced rate of the back-reaction with H_2 to regenerate the dihydride precursor must be one of the key factors making $Fe(dmpe)_2$ more reactive than $Ru(dmpe)_2$ toward C–H insertion reactions, particularly with alkanes and arenes.

Similar experiments involving photolysis of the ruthenium hydride place $Ru(PP_3)H_2$, in which the two bidentate dmpe ligands have given place to the tetradentate phosphine $PP_3 = P(CH_2CH_2PPh_2)_3$, reveal the

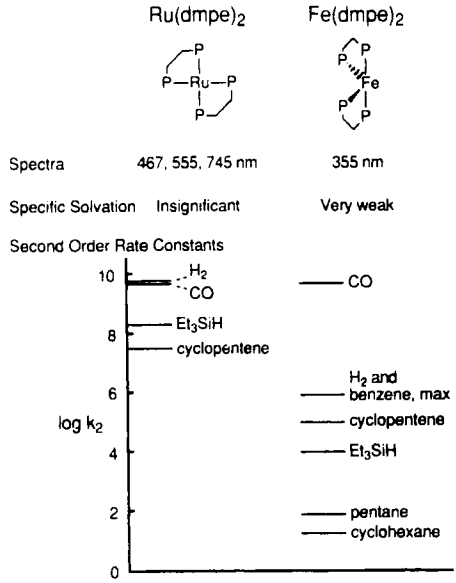

FIG. 17. Schematic comparison of the intermediates $Ru(dmpe)_2$ and $Fe(dmpe)_2$ (dmpe = $Me_2PCH_2CH_2PMe_2$) contrasting their UV-visible spectra and reactivities; the latter are expressed as log k_2 where k_2 is the second-order rate constant for reaction with the substrate at room temperature deduced by laser flash photolysis [reproduced with permission from (*61*), p. 364].

transient intermediate $Ru(PP_3)$ (*89*). Here the PP_3 ligand obliges the molecule to adopt not a square planar RuP_4 skeleton but a pyramidal (**XI**) or butterfly one (**XII**), and it is noteworthy that the UV-visible

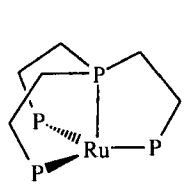

XI

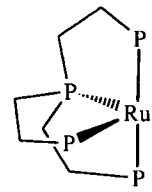

XII

spectrum resembles that of $Fe(dmpe)_2$ with but a single absorption at 395 nm. In its reactivity, moreover, $Ru(PP_3)$ is quite different from $Ru(dmpe)_2$, being much slower, for example, to react with H_2. The

corresponding osmium intermediate, which has a similar structure on the evidence of its UV-visible spectrum, does not even react with H_2 but inserts into the C–H bonds of alkanes with rate constants in the order of 10^5 $dm^3 \cdot mol^{-1} \cdot s^{-1}$ at 295 K. Hence, it appears that the enforced nonplanar geometry effectively prepares $Ru(PP_3)$, and more especially $Os(PP_3)$, for C–H activation (*89*).

In the first application of ultrafast TRIR spectroscopy (that is, with time-scales of 10^{-13} to 10^{-9} s), reductive elimination and oxidative addition of H_2 have been traced following flash photolysis of the related ruthenium carbonyl dihydride complex $Ru(PPh_3)_3(CO)H_2$ in benzene solution (*90*). This precursor is of particular note because it is known to catalyze insertion of alkenes into C–H bonds at the unsaturated carbon center of alkenes or arenes in a position β to a carbonyl group. The course of events has been monitored from excitation with an ultrafast UV laser (giving pulses at λ = 304 nm with an energy of 1–2 μJ, a full width of 4 ps at half of maximum duration, and a repetition rate of 1.05 kHz) to 2000 ps after the laser pulse using the ν(C–O) mode as a reporter, IR absorption measurements being made with a CO laser or with a diode laser via a detection system employing "up-conversion." Photolysis results in reductive elimination of H_2 and the formation of an unsaturated transient, $Ru(PPh_3)_3(CO)$, which can be identified unequivocally on the basis of its rapid build-up, the kinetics of its reaction with H_2, the partial regeneration of starting material, and the frequency of its ν(C–O) band. Moreover, the photoelimination step—involving H–H bond formation, Ru–H bond cleavage, and any reorganization of the coordination geometry at ruthenium—is found to be complete within 6 ps.

Nor has the speed limit yet been reached, for there are even ways of clocking chemical events at the femtosecond level. For example, Ahmed Zewail and his colleagues at the California Institute of Technology have developed a novel approach relying on ultrafast lasers giving femtosecond pulses to study in real time the transition-state dynamics of charge-transfer and other reactions (*91*, *92*). The entire molecular system is prepared on a reactive potential energy surface and in a well-defined impact geometry. A femtosecond light pulse induces a charge-transfer transition, and the dynamics of the ensuing events are then followed by interrogating the transition state or the reaction products; this is done with probe femtosecond light pulses causing photoionization and mass spectrometric sensing of the resulting fragments. The method is well illustrated by the dissociative charge-transfer reaction of the benzene-iodine complex (*91*):

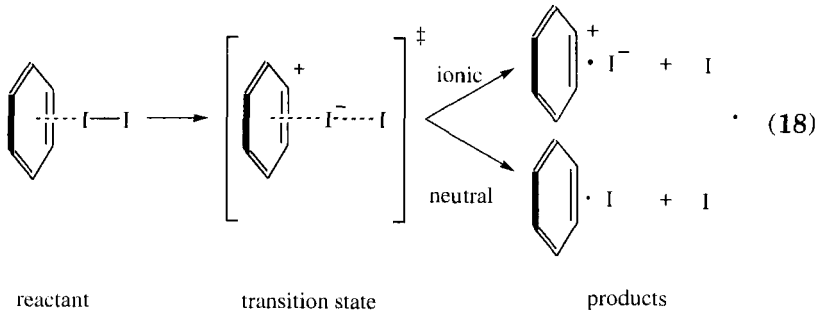

(18)

The transition state is directly accessed by excitation into the charge-transfer absorption band of the complex formed initially by expanding a gas mixture containing benzene, iodine, and helium through a pulsed valve. The resulting molecular beam is skimmed and intersected by the femtosecond laser pulses in the acceleration region of a linear time-of-flight mass spectrometer. The pulses of the femtosecond pump-laser (at λ = 275 nm) initiate the reaction and define t = 0. The probe pulses (at λ = 304.7 nm) then detect the free iodine atoms through a resonantly enhanced multiphoton ionization (REMPI) process. Transient I atom growth is measured by monitoring the I^+ signal as a function of the pump-probe delay. In addition, by using linearly polarized pump pulses and having provision for varying the orientation of the plane of polarization with respect to the axis of the mass spectrometer, it is possible to analyze the velocity distributions of the I atoms. Hence, microscopic elucidation of the reaction dynamics and mechanism becomes a practical proposition. We are able to witness the evolution and decay of the transition state and to show that dissociation with the formation of I atoms occurs via one of two exit channels. One (ionic) follows the ionic potential of the charge-transfer state $C_6H_6^+I_2^-$ to produce $C_6H_6^+ \cdot I^-$ + I; the other (neutral) involves intermolecular electron transfer through coupling of the transition state to neutral, locally excited, iodine-repulsive states, and in this case the products are $C_6H_6 \cdot I$ + I. With a timescale of 250 fs, the neutral process is ultrafast, outstripping the ionic process, which proceeds at a leisurely 800 fs or so. The kinetic energy characteristics of the I atoms even go so far as to reveal a near-axial geometry for the *transition state.* A similar approach has been adopted to show that the two-center elimination reaction (*19*) is a two-step, nonconcerted process evolving via the intermediate C_2F_4I (*92*):

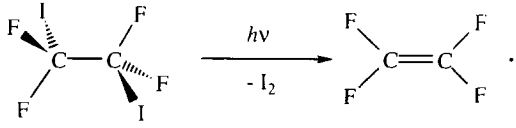

(19)

Here the time-scales for the breaking of the two C–I bonds differ by two orders of magnitude: the *primary* step takes about 200 fs, whereas the *secondary* step occupies 25 ps. The speed of the first step reflects the repulsive force in the C–I bond caused by the promotion of a nonbonding electron from the highest occupied molecular orbital (HOMO) to the σ^* lowest unoccupied molecular orbital (LUMO), whereas the second elimination is governed by the energy redistribution attending the concerted fission of a C–I σ-bond and making of a C–C π-bond.

The high-resolution spectroscopic methods involving, for example, infrared diode lasers that have been successfully applied to the detailing of gaseous transients have also been adapted to the time domain (*10*). High temporal resolution cannot of course be reconciled with high spectral resolution, but measurements made at even millisecond or microsecond intervals can still provide invaluable information about many reaction systems, with the bonus of unambiguous identification of intermediate species made possible by the high spectral definition. Reactions have been induced typically by irradiation with a high-power source, such as an excimer or CO_2 laser, or on occasion by pulse radiolysis, and the subsequent course of events has been monitored by a suitable high-resolution spectroscopic probe. For example, Curl's group at Rice University in Houston, Texas has investigated the reaction between the radicals NH_2 and NO, which appears to proceed via more than one channel (*93*):

$$\mathrm{NH_2 + NO} \longrightarrow \begin{cases} \mathrm{N_2 + H_2O} & \text{(a)} \\ \mathrm{H + N_2 + OH} & \text{(b)} \\ \mathrm{HN_2(?) + OH} & \text{(c).} \end{cases} \qquad (20)$$

This is of considerable interest because of the key role of the reaction in the thermal "de-NO_x" process involving the catalyzed reaction of ammonia with nitrogen oxides; hence, in principle, the gaseous emissions from industrial plants and power stations can be purged of the

noxious oxides, which are known to be major sources of smog and acid rain. Reaction (20) can be initiated by excimer laser photolysis of ammonia in the presence of NO and monitored by comparing the intensity of the infrared absorption due to NH_3 with that due to NH_2 as functions of time, and also with those due to OH and H_2O. Hence, the branching ratio of the OH channel or channels has been determined at different temperatures, with results suggesting that an additional channel may be implicated.

Replacing the probe laser of these studies with electron pulses offers a means of imaging structural changes by electron diffraction, but observation of chemical changes in this way is nontrivial, and only recently have the odds against the experiment been significantly shortened (*94–96*). The essential experimental principles of "stroboscopic" electron diffraction were first devised more than a decade ago, with a pulsed electron beam being generated by photoemission with millisecond to picosecond time resolution. Major advances have come with the application of online data-recording techniques, involving either photodiode array or charge-coupled device (CCD) detection. Quite apart from the low intensity of coherent molecular scattering compared with incoherent background scattering, however, numerous problems remain to be solved. How, for example, is one to determine *in situ* the zero of time in a chemical change? And how is one to take account of molecular ensembles in nonequilibrium (that is, non-Boltzmann) vibrational distributions? In fact, a temporal resolution of 15 ns has been achieved with a pulsed laser-driven electron source. Hence, the structural and vibrational kinetics of CS have been explored during the first 120 ns following the photodissociation of CS_2 at $\lambda = 193$ nm (*94*):

$$CS_2(X^1\Sigma_g^+) \xrightarrow{\lambda = 193\,\text{nm}} CS_2(^1B_2{}^1\Sigma_u^-) \rightarrow CS(X^1\Sigma^+) + S(^3P_J \text{ or } ^1D_J). \quad (21)$$

The observed changes of vibrational population with time have been interpreted on the basis of inelastic collisions of CS with sulfur atoms in the electronically excited ^1D state. Further hazards await any attempts to probe picosecond or subpicosecond changes by electron diffraction: space–charge effects broaden the electron pulse-width, and temporal overlap of the initiating photon pulse and the probe electron pulse must somehow be established. For ultrafast studies it is necessary then (i) to measure the electron pulse-width, (ii) to have the means of accurate clocking of the reaction, and (iii) to be able to detect *single* electrons (so as to reduce the electron flux and minimize space–

charge broadening). Zewail and his group have risen to this challenge by developing the new apparatus shown in Fig. 18 (*96*). This consists of a femtosecond laser, an ultrafast electron gun, a free-jet expansion source, and a newly designed two-dimensional single-electron detec-

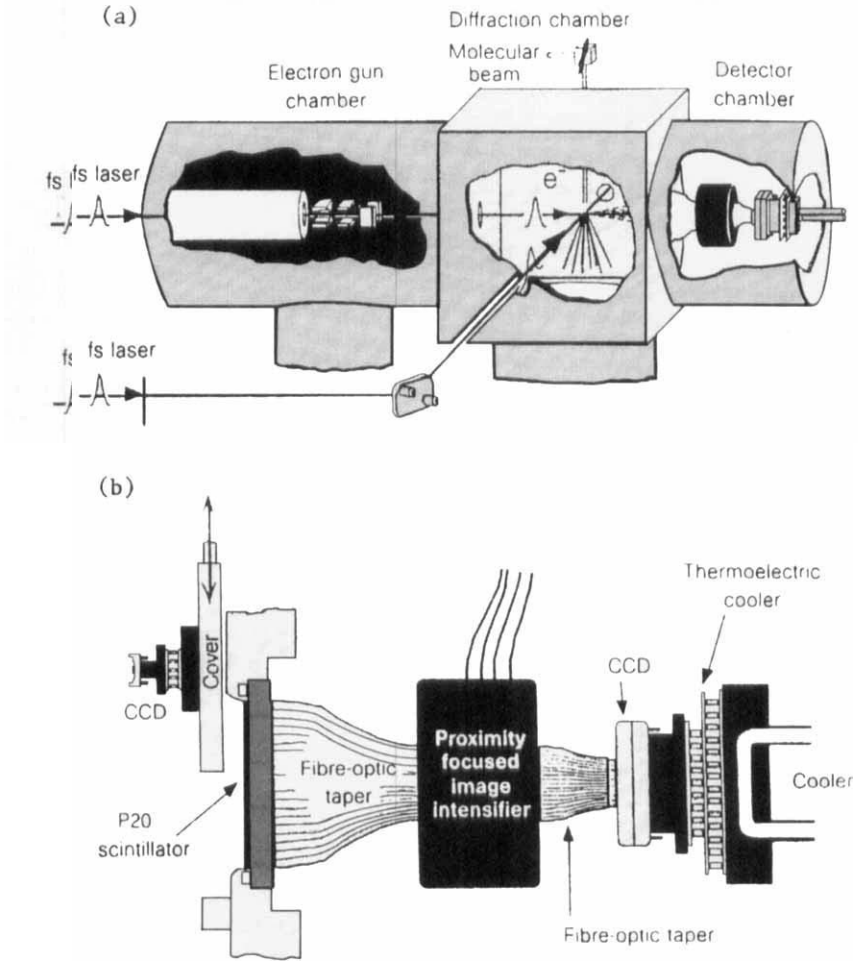

FIG. 18. (a) Ultrafast electron diffraction apparatus consisting of an electron gun chamber, a diffraction chamber, and a detector chamber. Two fs laser pulses are used, one to initiate the chemical change and the second to generate the electron pulse. (b) Detector system: incident electrons either directly bombard a small CCD or strike a phosphor-coated fused fiber-optic window. Light emitted from the phosphor is amplified by an image intensifier and brought to a scientific-grade CCD. Both CCDs are thermoelectrically cooled [reproduced with permission from (*96*), p. 160].

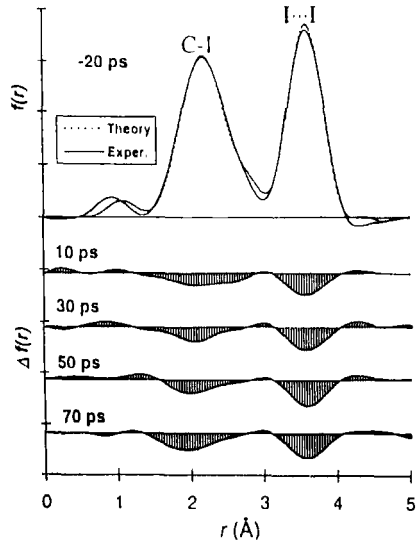

FIG. 19. Radial distribution functions $f(r)$ and $\Delta f(r)$ derived from the molecular scattering curves for gaseous CH_2I_2 at different delay times between the photodissociating fs laser pulse (at λ = 310 nm) and the ps electron pulse (pulse-width 15 ps). The corresponding theoretical $f(r)$ curve for CH_2I_2 is superimposed on the −20-ps data set. The changes observed are at r = *ca.* 2.0 and 3.5 Å corresponding to the C—I and I···I internuclear spacings, respectively [reproduced with permission from (*96*), p. 161].

tion system. Femtosecond laser pulses are created from a colliding-pulse mode-locked ring dye laser, the output from which is directed through a four-stage pulsed dye amplifier with no pulse compression (620 nm, 2–3 mJ, 30 Hz, 300 fs). To initiate the reaction, 95% of this beam is doubled (310 nm, *ca.* 250 μJ); the remainder (also doubled) is focused on a back-illuminated, negatively biased photocathode to generate the electron pulses. Critical to the success of the experiment is the detector, a two-dimensional CCD operating in a direct electron bombardment mode. Hence, a temporal resolution in the picosecond range can be realised. The first such studies have monitored the photodissociation of CH_2I_2 at λ = 310 nm; the molecular scattering and radial distribution functions vary significantly with time (see Fig. 19, for example) in a manner wholly consistent with Reaction (22):

$$CH_2I_2 \xrightarrow{h\nu} CH_2I + I. \qquad (22)$$

A more detailed quantitative analysis may be expected to elucidate the structure of the CH_2I intermediate. Modulation and difference detection techniques should provide a way of suppressing the background scattering from unreactive species, thereby enhancing the precision with which structure changes can be evaluated.

To understand the whole of a photochemical pathway requires a knowledge of the excited electronic state or states (*75*, *97*). In addition, some thermally activated processes proceed through the formation of intermediates or of products in excited states (witness, for example, the formation of singlet dioxygen). However, inorganic and organometallic molecules in these states are generally far too short-lived to be characterized *directly* by conventional spectroscopic observations, and there is no physical device open to us that will significantly extend their lifetimes. Figure 20 illustrates schematically a simple system involving just the ground and one excited state, and

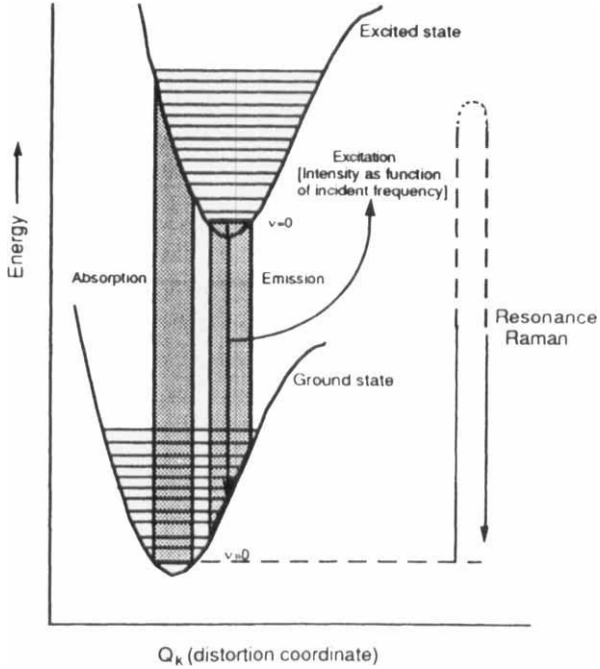

FIG. 20. Schematic representation of the potential energy curves for the ground and an excited electronic state of a molecule and some of the spectroscopic connections that can be made between them [reproduced with permission from (*75*), p. 119].

some of the spectroscopic connections that can be made between them. In principle, the optical absorption and excitation spectra provide a means of probing the vibrational levels of the *excited* state, whereas the emission spectrum reports not only on the vibrational levels of the *ground* state but also on the *lifetime* of the excited state. The intensities of the vibrational components of these spectra contain the seeds of information about the distortion the molecule experiences with the switch from the ground to the excited state. Unfortunately, though, relatively few molecules, and then at low temperatures, afford the sort of fine structure needed to make this a realistic proposition. The metallocene intermediates $(\eta^5\text{-}C_5H_5)_2M$ (M = W or Re) provide two cases in point, well-resolved vibrational progressions in the optical spectra of the matrix-isolated species admitting meaningful estimates of the changes in the metal–to–ring-centroid distance accompanying the electronic transition at lowest energy (*61*, *76*). Resonance Raman spectra also give access to similar structural information. The case of the binuclear iron carbonyls $(\eta^5\text{-}C_5R_5)_2Fe_2(CO)_4$ (R = H or Me) has already been alluded to (*85*), and similar studies have shown that the W–N and *trans* C–O bonds of $W(CO)_5$(pyridine) are extended by 18 and 12 pm, respectively, on excitation to the photoactive state (*75*). However, none of these methods involves probing of the excited state *in real time,* with the advantages this would bring to its structural and temporal delineation. One way of observing directly the vibrational spectrum of a molecule in an excited state is to engage TR^3 measurements (*80*), as with $W(CO)_4$(diimine) complexes (diimine = 2,2′-bipyridine or related species) in the tungsten-to-diimine charge-transfer excited state at lowest energy (*98*). The totally symmetric *cis*-carbonyl ν(C–O) mode has a frequency about 50 cm^{-1} higher than it does in the ground state, implying some reduction of metal–carbonyl π-back-bonding in the excited state. For all its merits, however, this approach is somewhat limited in its application, and there are real attractions in being able to record the infrared spectrum of a molecule in an excited electronic state. The new developments in TRIR spectroscopy now make this possible, at least in suitable cases. Thus, fast TRIR measurements are able to detect and monitor the lower metal-to-ligand charge-transfer state (MLCT where L = 4-cyanopyridine) of the tungsten pentacarbonyl complex $W(CO)_5$(4-cyanopyridine), **XIII** (*99*). Excitation causes the ν(C–O) infrared bands to shift to higher frequency, confirming that the metal center is oxidized in the excited state. This state can be observed to decay, partly reverting to the ground state and partly with dissocia-

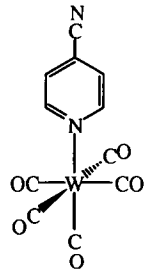

XIII

tion to form solvated $W(CO)_5$ and 4-cyanopyridine. The second reaction channel depends on rapid thermal equilibration between the MLCT and a second excited state, which is metal-centered or ligand field (LF) in nature, and it is this state that is dissociative with respect to separation of the 4-cyanopyridine ligand. Confirmation of this comes from the finding that the yield of $W(CO)_5$ varies with temperature, giving an estimate of some 4000 cm^{-1} for the energy gap separating the lowest MLCT and LF states (see Fig. 21). This example illustrates the sort of subtle details that time-resolved studies are now able to chart with regard to excited states and the chemical processes they beget.

About reactions occurring in the solid state there is not generally the same urgency that distinguishes so much of the chemistry of the more mobile phases. There may not be the same call for ultrafast

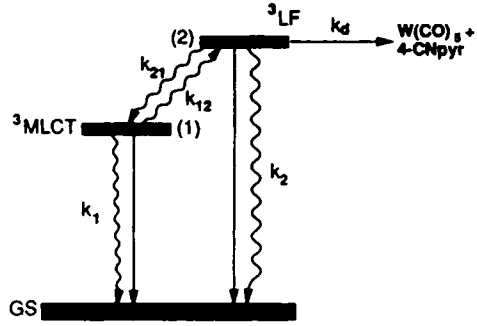

FIG. 21. Scheme showing the low-energy states of the photosystem $W(CO)_5$(4-CNpyr) (4-CNpyr = 4-cyanopyridine). k_1 and k_2 represent the sums of the radiative and nonradiative rate constants for the decay of the levels 1 and 2, respectively; k_d is the rate constant for photodissociation to $W(CO)_5$ and 4-CNpyr [reproduced with permission from (*99*), p. 3546].

methods of detection and analysis, but the ability to follow the evolution of a solid-state transformation is no less desirable for a proper kinetic and mechanistic understanding of the change. One such change currently attracting much interest is intercalation whereby mobile guest species enter a crystalline host lattice that contains an interconnected system of empty lattice sites (*100*). The staging of intercalation in $Ag_{0.17}TiS_2$ and Hg_xTiS_2 has been effectively witnessed, for example, as a function of time by high-resolution transmission electron microscopy. There has been developed, in addition, a reaction cell that enables intercalation reactions to be monitored *in situ* using real-time X-ray diffraction techniques. Exploiting the high flux, white X-ray radiation from a suitable synchrotron radiation source and energy-dispersive diffraction techniques permits a large energy window of the powder X-ray diffraction spectrum to be recorded simultaneously at a single fixed detector angle, with acquisition times in the order of seconds. Figure 22 illustrates strikingly (*100*) the progressive intercalation of the electron-rich metallocene $(\eta^5\text{-}C_5H_5)_2Co$ into a tin disulfide host. Still more dramatic is the very recent tour de force in protein science in which a group led by Michael Wulff and Keith Moffat at Chicago has virtually "watched" a protein function (*101*). Working at the European Synchrotron Radiation Facility, this team has devised a way of collecting pulsed Laue X-ray diffraction patterns with *nanosecond* time resolution. Hence, it has been possible to trace the structural changes that accompany the process of heme

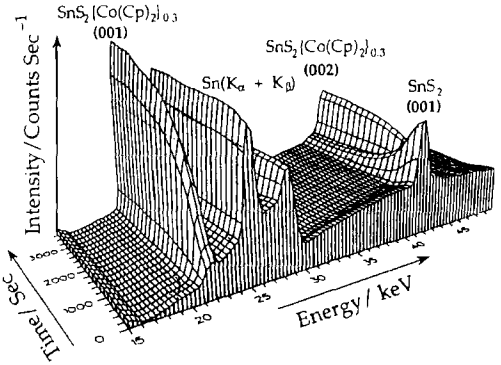

FIG. 22. A stack plot showing the evolution of the energy dispersive X-ray diffraction spectrum of SnS_2 following the injection of $(\eta^5\text{-}C_5H_5)_2Co$. Each spectrum took 10 s to record. The signals at 25 and 29 keV arise from resonances from the tin K_α and K_β core electrons and have been used to normalize the other signals [reproduced with permission from (*100*), p. 183].

and protein relaxation brought about first by photodissociation and then by rebinding of the carbon monoxide complex of myoglobin.

V. Experimental Characterization of Reaction Intermediates: Flow and Other Methods

The basis of flow methods has been outlined earlier. We have to find a way of generating our intermediate continuously in a flowing system—sometimes by mixing gases or solutions, sometimes by the action of a discharge—in a way that can be matched to its kinetic properties, the flow rate, and the time-scale of the spectroscopic method of detection. Even here it may be necessary to keep to a minimum the time taken to record the spectrum. In the past much of the work with flowing gases relied on photographic recording of electronic emission or absorption spectra, but only for the smallest molecules are these likely to give detailed information about the vibrational and other properties of any intermediates. By contrast, current laser techniques allow much more subtle interrogation of transient molecules, both small and large, in flow systems, leading sometimes to the identification and precise characterization of these molecules (*10*), as well as reporting on the kinetics of the reactions that feed upon them.

The sort of apparatus that has been used for the study of a gaseous reaction initiated by a discharge is shown schematically in Fig. 23 (*73*). The time between initiation and reactant or product detection at some point downstream in the flow tube can be calculated if the velocity of the gas mixture is known. Detection and monitoring of the relevant species can be effected by various spectroscopic techniques, usually mass spectrometry, resonance fluorescence, laser-induced fluorescence, ESR, or laser magnetic resonance; high-resolution techniques such as microwave and infrared diode laser spectroscopy are also compatible with the analysis of reactive gas flows, although they lack the sensitivity of the more widely used methods which are better suited to kinetic studies. Resonance fluorescence is a well-tried method for tracking the concentrations of atomic transients (e.g., H, N, O, F, Cl, or Br), whereas laser-induced fluorescence (LIF) offers greater sensitivity and applicability, especially for molecular transients (e.g., OH, CN, or CH_3O), at the cost of greater experimental complexity. Laser magnetic resonance (LMR) employs a CO_2 laser to produce a variety of sharp rovibrational lines to one of which a rovibrational line of a radical may often be tuned by the application of

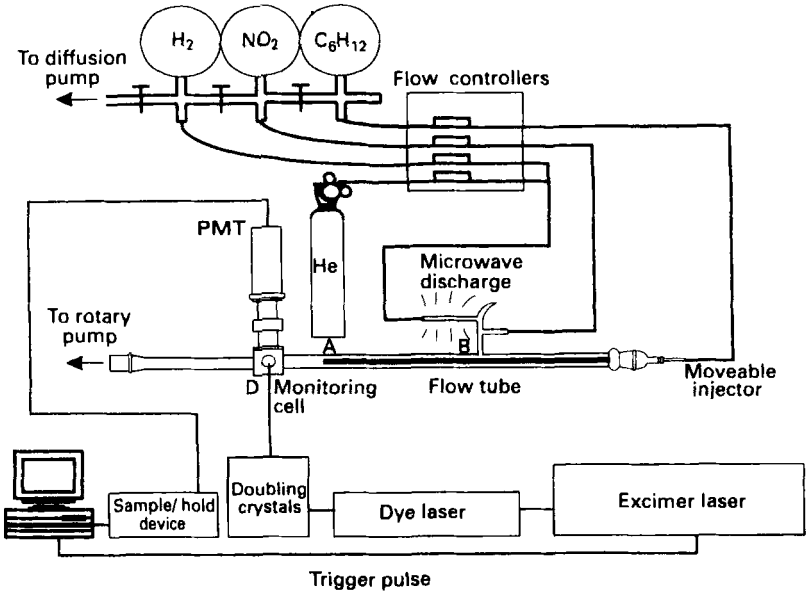

FIG. 23. Discharge flow apparatus used to study reactions of OH radicals with detection by laser-induced fluorescence. The OH radicals are generated *in situ* by the reaction between H atoms (themselves formed by the action of a microwave discharge on an H_2/He mixture) and NO_2. The distance between the points of initiation and detection is varied by moving the inlet tube [reproduced with permission from (*73*), p. 30].

a magnetic field. The biradical methylene is generated in its triplet electronic ground state by the reaction of oxygen atoms with ketene:

$$O + CH_2{=}C{=}O \rightarrow {}^3CH_2 + O{=}C{=}O. \qquad (23)$$

At slightly higher energies there exists a singlet state. Whereas singlet methylene can be detected by LIF, only the triplet state responds to LMR. Hence, it will be evident that the detection techniques are often complementary, and that no one technique is ideal for all transients. The reaction of ${}^3CH_2$ with ethene,

$$ {}^3CH_2 + CH_2{=}CH_2 \rightarrow CH_3CH{=}CH_2, \qquad (24)$$

has been studied by monitoring the LMR signal as a function of the distance between the mixing point and the laser detector with a range of different ethene concentrations; on this basis the relevant kinetic parameters have been evaluated (*73*).

Flow methods have found frequent application in the direct study of ClO radicals and related species noteworthy as sources and reservoirs of the halogens in the atmosphere (*17*). In a typical experiment an inert carrier gas is pumped at pressures near 1–10 torr down a glass or metal flow tube; the first reactant may be added at a point upstream to the carrier flow, and the second reactant is added subsequently. The evolution of concentration with distance after mixing is then followed. Hence, for example, the reactions of ClO generated in a discharge-flow system have been explored, and mass spectrometric measurements have been used to determine the overall rate constant for its decay by the second-order process [Eq. (25a)] (*102*); resonance fluorescence associated with Cl atoms indicates that Reaction (25b) is the major pathway by which ClO decays. Mass spectrometric detection has also been used to determine the relative importance of the two channels [Eq. (25c)] followed by the reaction between ClO and the NO_3 radical (*103*), whereas ESR detection of the ClO provides a means of exploring the kinetics of the reaction with HNO_3, which probably proceeds according to Eq. (25d), and so allows this to be discounted as having a significant role in the stratosphere (*104*).

$$\left.\begin{array}{lll} ClO + ClO \longrightarrow \text{all products} & (a) \\ ClO + ClO \longrightarrow Cl + ClOO & (b) \\ ClO + NO_3 \longrightarrow \begin{cases} ClOO + NO_2 \\ OClO + NO_2 \end{cases} & (c) \\ ClO + HNO_3 \longrightarrow HCl + NO_2 + O_2. & (d) \end{array}\right\} \quad (25)$$

Flow methods are not without their limitations (*73*). In practice they are usually limited to reactions with time-scales no shorter than the millisecond range. Reactions involving more than one reagent pose particular problems through the time taken for efficient mixing to occur—in the order of a fraction of a millisecond at a gas pressure of about 1 torr. A further restriction on kinetic studies is the need to retain a uniform flow velocity along the entire cross section of the tube. In fact, these conditions of "plug flow" can be attained only at low pressures, so flow experiments are generally restricted to gas pressures below 10 torr. There are also the seeds of potential compli-

cations in unwanted heterogenous reactions occurring at the walls of the flow tube that may catalyze the reaction under investigation, promote secondary reactions, or scavenge the reaction intermediates.

Most flow studies have been directed toward the kinetic elaboration of the reactions of intermediates that have been characterized previously by independent means. However, the flow method has also been exploited rather differently to help elicit detailed structural and spectroscopic properties of numerous molecules and molecular ions having but a fleeting existence under normal conditions. Hirota and his group at the Institute for Molecular Science at Okazaki have worked wonders with a flow reactor, using discharge, thermal, or photolysis methods to generate the transients and typically surveying the rotational or rovibrational spectrum of the flowing vapor at high resolution by a microwave or tunable infrared diode laser probe (*10*). The methods of production and sampling depend on the lifetime of the transient—that is, whether it is generated inside or outside the cell and how fast it must be pumped through the cell to create a workable effective pathlength for absorption spectroscopy. Instead of probing the flowing gas *laterally* for information about changes of composition with distance, the practice now is usually to probe the gas column *longitudinally* so as to intercept as many molecules as possible, and often with multipass facilities to give optical pathlengths of tens of meters. For example, the NO_3 radical—a prominent player on the atmospheric scene—has been generated in a flow system by admixing NO_2 with an excess of O_3 and characterized by its antisymmetric N–O stretching mode (ν_3) by means of a tunable infrared diode laser spectrometer (*105*). Here Zeeman modulation turns out to be invaluable in picking out the absorption lines due to paramagnetic NO_3 from among the many lines due to diamagnetic species. The results indicate that NO_3 is planar and conforms to D_{3h} symmetry in the $^2A_2'$ ground electronic state with an N–O bond length of 124.0 pm. On the other hand, close scrutiny reveals some intriguing anomalies, possibly arising from interaction between the ground state and a neighboring $^2E'$ excited state. The transient $SiCl_2$, an intermediate in various chemical processes, has also been generated chemically (by passing $SiCl_4$ vapor over heated silicon powder) and characterized in a flow reactor by both LIF and microwave studies. The microwave measurements fix the equilibrium structure of the molecule with remarkable precision, giving r_e(Si–Cl) = 206.531 pm and $\angle$Cl–Si–Cl = 101.324°, together with harmonic, cubic, and third-order anharmonic potential constants (*106*).

Flow systems are not limited to the study of gaseous reactions, and with certain alterations can be applied to the study of reactions in the liquid phase (*3*, *73*). Because mixing is significantly slower in the liquid phase, attention has to be paid to the design of the mixing chamber, which may include, for example, an elaborate set of baffles to promote turbulent flow and mixing of two reactant solutions. A familiar and more economical variation on the flow theme is the stopped-flow technique. As with continuous flow, the reactant solutions are injected from syringes into a mixing cell, whence the mixture flows into an observation tube. After a few milliseconds the flow is abruptly arrested. The real-time evolution of the species present in solution is then monitored; in effect, the method is exactly analogous to conventional batch-mixing kinetic studies and the stopped flow is simply a device for the rapid mixing of two solutions. The most common detection technique is electronic absorption spectrophotometry, a relatively blunt instrument when it comes to the identification and characterization of reaction intermediates in the condensed phases. No better examples of the use of stopped-flow methods can be found than in the work of Dale Margerum and his colleagues at Purdue University, who have developed a pulsed-accelerated-flow spectrophotometer with UV-visible detection that permits the measurement of pseudo-first-order rate constants as large as $5 \times 10^5\ s^{-1}$ ($t_{1/2} = 1.4\ \mu s$) (*107*). Typical of the kinetic studies carried out by this group on a wide range of "classical" inorganic reactions in aqueous solution are those implying (i) that hydroxylamine is oxidized by iodine by way of the adduct $I_2 \cdot NH_2OH$, which undergoes general-base-assisted deprotonation to give the intermediate INHOH (*108*), and (ii) that bromide ions are oxidized by nitrogen trichloride through the intermediate agency of $NBrCl_2$ (*109*). Here we are relying on kinetic measurements mainly, if not exclusively, for whatever inferences may be drawn about reaction intermediates. In contrast to the gas phase, solutions labor under the disadvantage that kinetic measurements are confined to a relatively narrow temperature range, normally 40°C or less, thereby impairing the precision of any estimates of activation parameters. Indeed, recent years have seen a perceptible trend away from attempting any such estimates.

From our present perspective, though, no level of confidence in reaction rates can entirely redeem the uncertainties that are apt to cloud the identities of any transients stopped-flow and related studies may disclose, whether directly or indirectly. For example, stopped-flow experiments have been carried out to study the reaction occurring in

aqueous solution between cerium(IV) and an excess of peroxotitanium(IV), $Ti(O_2)^{2+}$ (*110*). This yields a transient, which, on the evidence of its ultraviolet absorption spectrum, conditions of formation, and decay properties, was believed to be a superoxo–titanium(IV) species existing apparently in two forms that were tentatively formulated as $Ti(OO)^{3+}$ and $Ti(OO)OH^{2+}$. A separate investigation of the decomposition kinetics of this species suggests that it is more likely to be $TiO(HO_2\cdot)^{2+}$, that is, a complex of the aquated TiO^{2+} ion with the perhydroxyl radical (*110*). ESR measurements may shed a more distinctive light on paramagnetic intermediates. Thus, the oxidation of chromium(III) to chromium(VI) by hydrogen peroxide in basic media occurs via a branching mechanism: from the initial formation of a chromium(III)–peroxide intermediate, one pathway leads to a chromium(IV) intermediate and a second pathway leads to a chromium(V) intermediate, which can be identified empirically by its ESR spectrum (*111*). Nevertheless, doubts assailing us about the true nature of intermediates like these contrast starkly with the conviction high-resolution studies bring to the identification and characterization of a gaseous intermediate like $SiCl_2$.

For all its immense power and versatility, NMR spectroscopy has kept a relatively low profile in the story so far. There is no doubting the potential of real-time NMR measurements to report directly on a reaction and on all the components of the reaction mixture. There are certainly ways of allying rapid mixing, stopped-flow, temperature-jump or other methods with NMR detection (*3*, *112*), but no technical stratagem can remedy the want of sensitivity that is inherent in the NMR experiment. Nevertheless, the ability of the technique specifically to monitor a free ligand can be turned to good account, for example to resolve the three stages in the displacement of three dmso molecules (dmso = Me_2SO) in the cation $[Al(dmso)_6]^{3+}$ by one terdentate ligand 2,2′: 6′2″-terpyridine (terpy), **XIV**, in nitromethane solution (*113*). The implication is that there are two intermediates involving

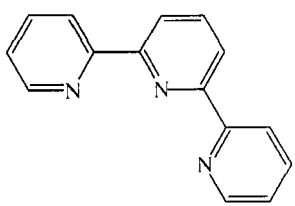

XIV

mono- or bidentate coordination of the terpy ligand to the metal center. Rates for the three stages have been determined using a special stopped-flow apparatus, with ^1H NMR measurements reporting on the release of coordinated dmso molecules. Hence, activation parameters have been determined for the first bond formation and the two slower chelate-ring closures that ensue. More recent experiments have turned to the much more elaborate puzzle of protein folding, where NMR studies are privy to unique structural insights (*114*). The resulting spectra relay information not only about kinetic folding events but also about the structures of folding intermediates, partly folded states, peptide fragments, and unfolded or denatured proteins.

Recent developments in mass spectrometry, with "electrospray" ionization, provide another relatively fast device for monitoring solution processes in real time, and one that has been applied to the teasing problems of protein folding (*115*, *116*). Such folding is assisted by a host of helper proteins including the molecular chaperones, which are thought to safeguard newly synthesized proteins from unproductive interactions that may lead to aggregation. This raises the problem of how to determine the conformational properties of a relatively small substrate protein in the presence of a large chaperonin oligomer like GroEL. One new perspective shown schematically in Fig. 24 (*115*) seeks to elicit the information from hydrogen exchange protection (a technique that has revolutionized studies of protein folding *in vitro*) specifically relating to complexes relevant to folding in the cell. For example, a partially folded protein bound within the GroEL central cavity can be directly studied by electrospray ionization mass spectrometry (ESI-MS), allowing the visualization of both the GroEL subunits and the ligand in the same spectrum. When combined with hydrogen exchange labeling, this approach admits the study of individual components of the complex that retain the history of the complexed state by virtue of their deuterium content; it thus obviates the need to quench exchange and dissociate the complex before measurement. Hence, we are able in effect to measure selectively the protection of individual components in a mixture of species and in proteins that are well beyond the molecular mass range open to detailed NMR analysis, and also to observe states too short-lived to be characterized, say, by X-ray crystallography. In addition, differences in the cooperativity of folding events can be detected directly by the ESI-MS method (*116*).

Yet another option is being elaborated by Fraser Armstrong and his group at Oxford through fast-scan electrochemical techniques, which have now advanced to the point where they are capable of probing

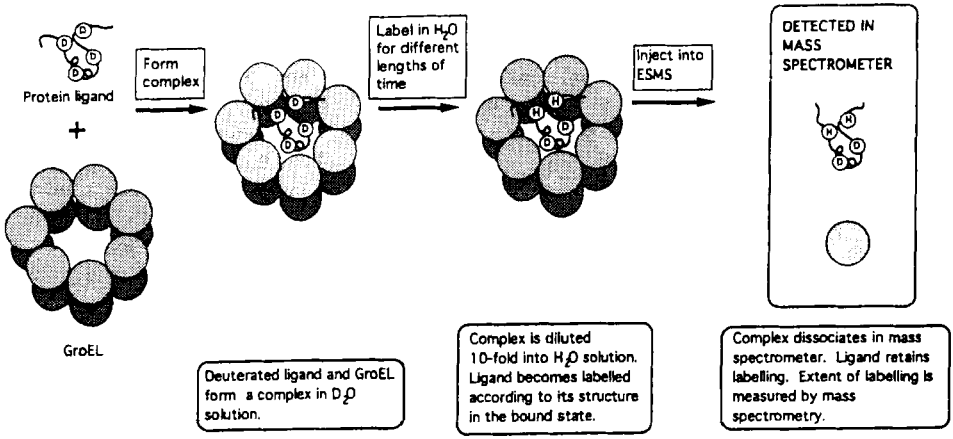

FIG. 24. Schematic diagram outlining the experiment designed to monitor hydrogen exchange in the GroEL: [3SS] BLA complex (BLA = bovine α-lactalbumin) by electrospray ionization mass spectrometry (ESI-MS). Before formation of the complex, all exchangeable sites in α-lactalbumin were deuterated by incubation of the apoprotein in D_2O. Hydrogen exchange is initiated by a 10-fold dilution of the complex in H_2O, pH 5.0, at 4°C. Dissociation of the GroEL into monomers in the gas phase releases the bound polypeptide ligand while maintaining the protection in the substrate protein. In this way, the rate of hydrogen exchange of [3SS] α-lactalbumin (and GroEL) in the complex can be measured directly as a change in their masses as a function of the incubation time in H_2O by ESI-MS [reproduced with permission from (*115*), p. 647].

transient intermediates formed during redox reactions (*117*). In the technique of "protein-film voltammetry," the redox protein molecules under investigation are adsorbed on the rotating electrode surface of a voltammetric assembly and interrogated there electrochemically. Cyclic voltammetry at scan rates up to 1000 $V \cdot s^{-1}$ may then reveal pairs of oxidation–reduction peaks, which may serve as markers by which the status of redox centers within the protein can be identified and quantified. In effect, we have an interactive "spectrum," albeit one providing no structural information; for that we must turn to true spectroscopic methods, such as ESR, to examine the species generated in solution at the appropriate potentials. Protein-film voltammetry has already been successfully exploited to track active-site redox transformations over a range of conditions and so reveal the intramolecular electron relays operating in the multicentered enzyme. Large systems like these hold out little prospect of furnishing the sort of structurally explicit information that is now available for simple molecules like Si_2H_2 or $Cr(CO)_5$. On the other hand, what we lose in struc-

tural definition may well be compensated by a clearer perception of the thermodynamic and kinetic properties that determine the reactivity of a given intermediate.

Problems of reliable identification are no strangers to studies that concentrate on kinetics, whether they involve the stopped-flow technique, relaxation methods, or other strategies. We may know very well the speed and order of a particular reaction; we may even be well versed in the dependence of the kinetic parameters on various conditions; however, we cannot always be sure of the exact nature of the reagents and the products, still less the intermediates formed on the way. To that extent, any mechanistic interpretation is bound to be impaired. Indeed, the situation has something of the surreal about it, reminiscent of the conversation between Alice and the Cheshire Cat:

> "Would you tell me, please, which way I ought to go from here?" "That depends a good deal on where you want to get to," said the Cat. "I don't much care where . . . ," said Alice. "Then it doesn't matter which way you go," said the Cat. ". . . So long as I get *somewhere*," Alice added as an explanation. "Oh, you're sure to do that," said the Cat, "if you only walk long enough."
>
> Lewis Carroll, "Alice's Adventures in Wonderland"

VI. Conclusions

In this account we have sought to highlight reaction intermediates and the crucial bearing they have on the way chemical processes actually take place. We have concentrated on how such intermediates can be directly observed, identified, characterized, and tracked by their spectroscopic properties. Frustration of the reactions to which the intermediates are natural prey can be achieved by control of temperature, pressure, and environment, and in these circumstances it may be perfectly possible to form a clear and detailed picture of a given intermediate on the basis of the same sort of spectroscopic methods that are used to study normal, long-lived species. To chart the *chemistry* of such an intermediate requires a closer acquaintance with the reality of normal conditions, and at least some concession not only to mobility, concentration, and temperature, but also to *time* as a variable; this commonly involves some form of time-resolved spectroscopic

probe, as in flash photolysis, or the induction of reaction not in a static but in a uniformly flowing gas or liquid.

A recurring example has been chromium pentacarbonyl, $Cr(CO)_5$, an intermediate most easily generated photochemically en route to substitution products of chromium hexacarbonyl (*60*, *61*). Matrix-isolation experiments were the first to fix the structure of this molecule and to alert us to its extraordinary reactivity. Experiments with fluid samples were then needed to elaborate on the ability of $Cr(CO)_5$ to bind supposedly inert molecules such as Xe, H_2, and CH_4, and time-resolved spectroscopy has opened our eyes to the energetics of these interactions as well as the photochemistry and kinetics of the processes involving $Cr(CO)_5$. So strongly is $Cr(CO)_5$ solvated that it is hard to conceive of the molecule in solution without its "token" ligand. Naked $Cr(CO)_5$ plays a role, it is true, but certainly does not live long enough to "wait" for a collision in dilute solution; instead, in the space of picoseconds, it picks up a token ligand from within its solvent cage via the pseudorotation illustrated in Fig. 13. Hence, the orthodox notion of a simple dissociative mechanism for a substitution reaction starting from saturated 18-electron $Cr(CO)_6$ and involving the intermediate formation of an unsaturated 16-electron intermediate must give place to an interchange model that is altogether more intricate and subtle and in which the solvent is no mere spectator. Even now, for all our knowledge of the chemistry of $Cr(CO)_5$ at time-scales of a nanosecond and longer, controversy and doubts continue to surround the very fast processes implicating the fragment.

No less striking have been the advances made in our understanding of the substitution reactions peculiar to the much studied binuclear iron carbonyl, **VIII** (*83–85*). Here, too, a variety of experimental techniques has been brought to bear on the intermediate photoproducts—one a binuclear species **IX** and the other a mononuclear radical **X**—which differ hugely in their reactivity.

The ability of a reaction intermediate such as $Cr(CO)_5$ to bind methane may be counterintuitive but commands attention for its significance in relation to C–H bond activation, a teasing but vital issue in the context of the chemical industry (*118*). Numerous complexes of alkanes with unsaturated transition-metal fragments (including atoms and ions) have now been detected in both the gas and condensed phases. It is not surprising that all of them are unstable at room temperature. Experiments in which alkanes undergo oxidative addition to, or reductive elimination from, transition-metal complexes have revealed, nonetheless, the intermediacy of alkane complexes.

For example, TRIR studies of liquid xenon solutions of the rhodium complex (η^5-C_5Me_5)$Rh(CO)_2$ witness on photolysis the expulsion of CO and formation of a transient characterized by its ν(C–O) mode; a similar band is observed at much the same frequency when liquid krypton is used as the solvent but belongs to a considerably more reactive carrier (*119*). The transients are most likely to be (η^5-C_5Me_5)Rh(CO)(Xe) and (η^5-C_5Me_5)Rh(CO)(Kr), respectively. In the presence of a small amount of cyclohexane, however, the intermediates transform rapidly into the insertion product (η^5-C_5Me_5)Rh(CO)(C_6H_{11})(H). The kinetics of formation of this product in liquid krypton are consistent not with a dissociative mechanism but with a reaction scheme incorporating an equilibrium between krypton and cyclohexane complexes of (η^5-C_5Me_5)Rh(CO) prior to oxidative addition. The failure to observe a distinct ν(C–O) mode for the alkane complex (η^5-C_5Me_5)Rh(CO)(C_6H_{12}) is probably due to overlap with the corresponding band of the krypton complex. Unambiguous though the case for transition-metal alkane complexes may be on the evidence of these and many other studies (*118*), the mode of coordination of the alkane has yet to be fathomed properly. Plainly these are but the early stages of a mechanistic expedition that is likely to take many years to complete.

In very different territory we have noted how a molecule such as ClO that is normally short-lived in the laboratory is still capable of exercising a major influence on the fate of stratospheric ozone (*17*). There is particular interest, for example, in the dimerization of ClO and subsequent photolysis of the products [see Eqs. 25(a) and 25(b)] because these processes may have a marked impact on the ozone depletion of the atmosphere above the polar regions. Of especial note in this context has therefore been the first preparation of another labile molecule with the composition Cl_2O_2 by halogen exchange between gaseous $FClO_2$ and $AlCl_3$ (*62*, *120*); trapping in a solid noble-gas matrix enables this species to be identified as chloryl chloride, $ClClO_2$, **XV**, on the basis of its infrared and ultraviolet spectra. From the vibrational frequencies of four independent isotopomers, the known properties of related compounds, and the results of *ab initio* calculations, the following geometric parameters have been estimated: r(Cl–Cl) = 222 pm, r(Cl=O) = 144.0 pm, $\angle$Cl–Cl=O = 103.5°, and $\angle$O=Cl=O = 116.0°. What is intriguing about the photochemistry of this new isomer of Cl_2O_2 is that it decays under appropriate conditions not only to the more familiar peroxo form ClOOCl, **XVI**, but also to a third, photolabile isomer, chlorine chlorite, ClOClO, **XVII**. At room temperature and partial and total pressures of 1 and

4 torr, respectively, $ClClO_2$ has a half-life of 1 min. Matrix studies involving selective irradiation adduce the first evidence for a second

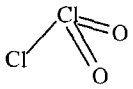

XV

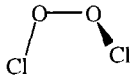

XVI

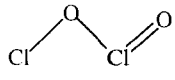

XVII

photodissociation channel disposing of ClOOCl (and giving 2ClO), and also make it clear that dimerization of ClO can lead to both ClOClO and ClOOCl. These results must surely be heeded by gas-phase kineticists and others seeking to model the atmospheric fates of the chlorine oxides.

"Everything's got a moral, if you can only find it," and to this tale there are not one but two morals. The first is that reaction intermediates, however ephemeral, can and should be explored directly. The second is that no one experimental or theoretical technique has a monopoly of the truth we seek; to arrive at a comprehensive and realistic picture the best policy must be to draw on as many sources as possible. It is true that the Promised Land of a proper understanding of the mechanisms of major chemical reactions is still a great way off and that the intermediates by which the reactions proceed are not going to be quick to yield up their secrets. However, it is equally true that without these secrets even the most inspired perceptions of mechanism are either incomplete or insecure. In Robin Perutz's trenchant words (*61*), "If you don't understand the intermediates, you don't understand the mechanisms."

> Not only is there but one way of *doing* things rightly, but there is only one way of *seeing* them, and that is, seeing the whole of them.
>
> J. Ruskin, "The Two Paths"

References

1. Tobe, M. L. "Inorganic Reaction Mechanisms"; Nelson: London, 1972.
2. Jordan, R. B. "Reaction Mechanisms of Inorganic and Organometallic Systems"; Oxford University Press: New York and Oxford, 1991.
3. Wilkins, R. G. "Kinetics and Mechanism of Reactions of Transition Metal Complexes"; 2nd ed., VCH: Weinheim and New York, 1991.
4. Darensbourg, D. J. *Adv. Organomet. Chem.* **1982,** *21,* 113.
5. Howell, J. A. S.; Burkinshaw, P. M. *Chem. Rev.* **1983,** *83,* 557.

6. Woodward, S. In "Comprehensive Organometallic Chemistry II," Vol. 5 (J. A. Labinger and M. J. Winter, Eds.), Chap. 4, pp. 215–280, Pergamon: Oxford, 1995.
7. Richter-Addo, G. B.; Legzdins, P. "Metal Nitrosyls"; Oxford University Press: New York and Oxford, 1992.
8. Niu, S.; Hall, M. B. *J. Am. Chem. Soc.* **1997,** *119,* 3077 and references cited therein.
9. (a) Seder, T. A.; Church, S. P.; Ouderkirk, A. J.; Weitz, E. *J. Am. Chem. Soc.* **1985,** *107,* 1432; (b) Fletcher, T. R.; Rosenfeld, R. N. *J. Am. Chem. Soc.* **1985,** *107,* 2203.
10. (a) Hirota, E. "High-Resolution Spectroscopy of Transient Molecules"; Springer: Berlin, 1985; (b) Hirota, E. *Int. Rev. Phys. Chem.* **1989,** *8,* 171; (c) Hirota, E. *Annu. Rev. Phys. Chem.* **1991,** *42,* 1; (d) Hirota, E. *Chem. Rev.* **1992,** *92,* 141; (e) Hirota, E. *Ann. Rep. Prog. Chem., Sect. C, Phys. Chem.* **1994,** *91,* 3.
11. Cox, P. A. "The Elements: Their Origin, Abundance, and Distribution", pp. 93–126, Oxford University Press: Oxford, 1989.
12. Manson, E. L., Jr.; Clark, W. W.; De Lucia, F. C.; Gordy, W. *Phys. Rev. A* **1977,** *15,* 223.
13. Huber, K. P.; Herzberg, G. "Molecular Spectra and Molecular Structure. IV. Constants of Diatomic Molecules"; Van Nostrand Reinhold: New York, 1979.
14. Ram, R. S.; Bernath, P. F. *J. Mol. Spectrosc.* **1996,** *180,* 414.
15. Lorenz, M.; Agreiter, J.; Smith, A. M.; Bondybey, V. E. *J. Chem. Phys.* **1996,** *104,* 3143.
16. Bredohl, H.; Dubois, I.; Houbrechts, Y.; Nzohabonayo, P. *J. Mol. Spectrosc.* **1985,** *112,* 430.
17. (a) Wayne, R. P. "Chemistry of Atmospheres," 2nd ed., Clarendon Press: Oxford, 1991; (b) Wayne, R. P.; Poulet, G.; Biggs, P.; Burrows, J. P.; Cox, R. A.; Crutzen, P. J.; Hayman, G. D.; Jenkin, M. E.; Le Bras, G.; Moortgat, G. K.; Platt, U.; Schindler, R. N. *Atmos. Environ.* **1995,** *29,* 2677.
18. Anderson, J. G.; Toohey, D. W.; Brune, W. H. *Science* **1991,** *251,* 39.
19. (a) Cohen, E. A.; Pickett, H. M.; Geller, M. *J. Mol. Spectrosc.* **1984,** *106,* 430; (b) Burkholder, J. B.; Hammer, P. D.; Howard, C. J.; Maki, A. G.; Thompson, G.; Chackerian, C., Jr. *J. Mol. Spectrosc.* **1987,** *124,* 139; (c) McLoughlin, P. W.; Park, C. R.; Wiesenfeld, J. R. *J. Mol. Spectrosc.* **1993,** *162,* 307.
20. Herzberg, G.; Johns, J. W. C. *Proc. Roy. Soc.* **1967,** *298A,* 142.
21. Kawaguchi, K. *J. Chem. Phys.* **1992,** *96,* 3411; *Can. J. Phys.* **1994,** *72,* 925.
22. Kawashima, Y.; Kawaguchi, K.; Hirota, E. *J. Chem. Phys.* **1987,** *87,* 6331.
23. Ebsworth, E. A. V.; Rankin, D. W. H.; Cradock, S. "Structural Methods in Inorganic Chemistry," 2nd ed., pp. 334–343, Blackwell Scientific Publications: Oxford, 1991.
24. See, for example, Blake, A. J.; Brain, P. T.; McNab, H.; Miller, J.; Morrison, C. A.; Parsons, S.; Rankin, D. W. H.; Robertson, H. E.; Smart, B. A. *J. Phys. Chem.* **1996,** *100,* 12280.
25. Fujiwara, H.; Egawa, T.; Konaka, S. *J. Mol. Struct.* **1995,** *344,* 217.
26. Fujiwara, H.; Egawa, T.; Konaka, S. *J. Am. Chem. Soc.* **1997,** *119,* 1346.
27. Molnár, J.; Marsden, C. J.; Hargittai, M. *J. Phys. Chem.* **1995,** *99,* 9062.
28. Hedberg, K.; Hedberg, L.; Bühl, M.; Bethune, D. S.; Brown, C. A.; Johnson, R. D. *J. Am. Chem. Soc.* **1997,** *119,* 5314.
29. Carlowitz, M. V.; Oberhammer, H.; Willner, H.; Boggs, J. E. *J. Mol. Struct.* **1983,** *100,* 161.
30. Cleaver, W. M.; Späth, M.; Hnyk, D.; McMurdo, G.; Power, M. B.; Stuke, M.; Rankin, D. W. H.; Barron, A. R. *Organometallics* **1995,** *14,* 690.
31. Legon, A. C. *Chem. Br.* **1990,** *26,* 562.

32. Legon, A. C. In "Atomic and Molecular Beam Methods," Vol. 2 (G. Scoles, Ed.), pp. 289–308, Oxford University Press: New York, 1992.
33. Legon, A. C. *J. Chem. Soc., Chem. Commun.* **1996,** 109.
34. Bloemink, H. I.; Hinds, K.; Legon, A. C.; Thorn, J. C. *Chem. Eur. J.* **1995,** *1,* 17.
35. Bloemink, H. I.; Hinds, K.; Holloway, J. H.; Legon, A. C. *Chem. Phys. Lett.* **1995,** *245,* 598.
36. Campbell, E. J.; Kukolich, S. G. *Chem. Phys.* **1983,** *76,* 225.
37. Campbell, E. J.; Read, W. G. *J. Chem. Phys.* **1983,** *78,* 6490.
38. Bloemink, H. I.; Evans, C. M.; Holloway, J. H.; Legon, A. C. *Chem. Phys. Lett.* **1996,** *248,* 260.
39. Barnes, M.; Hajigeorgiou, P. G.; Kasrai, R.; Merer, A. J.; Metha, G. F. *J. Am. Chem. Soc.* **1995,** *117,* 2096.
40. Davies, P. B. *Chem. Soc. Rev.* **1995,** *24,* 151.
41. Hirahara, Y.; Ohshima, Y.; Endo, Y. *J. Chem. Phys.* **1994,** *101,* 7342.
42. Yamada, C.; Hirota, E. *Phys. Rev. Lett.* **1986,** *56,* 923.
43. Bogey, M.; Bolvin, H.; Demuynck, C.; Destombes, J. L. *Phys. Rev. Lett.* **1991,** *66,* 413.
44. Colegrove, B. T.; Schaefer, H. F., III. *J. Phys. Chem.* **1990,** *94,* 5593.
45. Cordonnier, M.; Bogey, M.; Demuynck, C.; Destombes, J.-L. *J. Chem. Phys.* **1992,** *97,* 7984.
46. Harper, W. W.; Ferrall, E. A.; Hilliard, R. K.; Stogner, S. M.; Grev, R. S.; Clouthier, D. J. *J. Am. Chem. Soc.* **1997,** *119,* 8361.
47. See, for example, (a) Davies, P. B.; Martineau, P. M. *J. Appl. Phys.* **1992,** *71,* 6125; (b) Naito, S.; Ito, N.; Hattori, T.; Goto, T. *Jpn. J. Appl. Phys., Part 1* **1994,** *33,* 5967; (c) Fukuzawa, T.; Obata, K.; Kawasaki, H.; Shiratani, M.; Watanabe, Y. *J. Appl. Phys.* **1996,** *80,* 3202.
48. Perutz, R. N. *Chem. Rev.* **1985,** *85,* 77.
49. Downs, A. J.; Pulham, C. R. *Adv. Inorg. Chem.* **1994,** *41,* 171.
50. Sawyer, D. T. "Oxygen Chemistry," pp. 156–158, Oxford University Press: New York, 1991.
51. (a) Almond, M. J.; Downs, A. J. *Adv. Spectrosc.* **1989,** *17,* 1–511; (b) Andrews, L., and Moskovits, M., Eds., "Chemistry and Physics of Matrix-Isolated Species," North Holland: Amsterdam, 1989.
52. Downs, A. J. In "Low Temperature Molecular Spectroscopy" (R. Fausto, Ed.), pp. 1–93, NATO ASI Series, Series C: Vol. 483, Kluwer: Dordrecht, 1996.
53. Bondybey, V. E.; Smith, A. M.; Agreiter, J. *Chem. Rev.* **1996,** *96,* 2113.
54. Chetwynd-Talbot, J.; Grebenik, P.; Perutz, R. N. *Inorg. Chem.* **1982,** *21,* 3647.
55. Tague, T. J., Jr.; Andrews, L. *J. Am. Chem. Soc.* **1994,** *116,* 4970.
56. Poliakoff, M.; Weitz, E. *Acc. Chem. Res.* **1987,** *20,* 408.
57. Crayston, J. A.; Almond, M. J.; Downs, A. J.; Poliakoff, M.; Turner, J. J. *Inorg. Chem.* **1984,** *23,* 3051.
58. Müller, J. *J. Am. Chem. Soc.* **1996,** *118,* 6370.
59. Fletcher, S. C.; Poliakoff, M.; Turner, J. J. *Inorg. Chem.* **1986,** *25,* 3597.
60. Turner, J. J. In "Photoprocesses in Transition Metal Complexes, Biosystems and Other Molecules. Experiment and Theory" (E. Kochanski, Ed.), pp. 125–140, NATO ASI Series, Series C: Vol. 376, Kluwer: Dordrecht, 1992.
61. Perutz, R. N. *Chem. Soc. Rev.* **1993,** *22,* 361.
62. Jacobs, J.; Kronberg, M.; Müller, H. S. P.; Willner, H. *J. Am. Chem. Soc.* **1994,** *116,* 1106.

63. Bell, T. W.; Haddleton, D. M.; McCamley, A.; Partridge, M. G.; Perutz, R. N.; Willner, H. *J. Am. Chem. Soc.* **1990,** *112,* 9212.
64. Poliakoff, M.; Turner, J. J. *Adv. Spectrosc.* **1995,** *23,* 275.
65. Van der Veken, B. J. In "Low Temperature Molecular Spectroscopy" (R. Fausto, Ed.), pp. 371–420, NATO ASI Series, Series C: Vol. 483, Kluwer: Dordrecht, 1996.
66. Upmacis, R. K.; Poliakoff, M.; Turner, J. J. *J. Am. Chem. Soc.* **1986,** *108,* 3645.
67. Duckett, S. B.; Haddleton, D. M.; Jackson, S. A.; Perutz, R. N.; Poliakoff, M.; Upmacis, R. K. *Organometallics* **1988,** *7,* 1526.
68. Turner, J. J.; Simpson, M. B.; Poliakoff, M.; Maier, W. B., II. *J. Am. Chem. Soc.* **1983,** *105,* 3898.
69. Howdle, S. M.; Healy, M. A.; Poliakoff, M. *J. Am. Chem. Soc.* **1990,** *112,* 4804.
70. (a) McHugh, M. A.; Krukonis, V. J. "Supercritical Fluid Extraction: Principles and Practice," 2nd ed., Butterworth-Heinemann: Boston, 1994; (b) Poliakoff, M.; Howdle, S. *Chem. Br.* **1995,** *31,* 118.
71. Walsh, E. F.; Popov, V. K.; George, M. W.; Poliakoff, M. *J. Phys. Chem.* **1995,** *99,* 12016.
72. Rathke, J. W.; Klingler, R. J.; Krause, T. R. *Organometallics* **1991,** *10,* 1350.
73. Pilling, M. J.; Seakins, P. W. "Reaction Kinetics"; Oxford University Press: Oxford, 1995.
74. Poliakoff, M.; Weitz, E. *Adv. Organomet. Chem.* **1986,** *25,* 277.
75. Turner, J. J. In "Photoprocesses in Transition Metal Complexes, Biosystems and Other Molecules. Experiment and Theory" (E. Kochanski, Ed.), pp. 113–123, NATO ASI Series, Series C: Vol. 376, Kluwer: Dordrecht, 1992.
76. Perutz, R. N. In "Low Temperature Molecular Spectroscopy" (R. Fausto, Ed.), pp. 95–124, NATO ASI Series, Series C: Vol. 483, Kluwer: Dordrecht, 1996.
77. El-Sayed, M. A., Tanaka, I., and Molin, Y., Eds., "Ultrafast Processes in Chemistry and Photobiology"; Blackwell Science: Oxford, 1995.
78. Farhataziz; Rodgers, M. A. J. "Radiation Chemistry—Principles and Applications"; VCH: New York, 1987.
79. Goldstein, S.; Czapski, G. *Inorg. Chem.* **1997,** *36,* 4156.
80. Tripathi, G. N. R. *Adv. Spectrosc.* **1989,** *18,* 157.
81. George, M. W.; Poliakoff, M.; Turner, J. J. *Analyst* **1994,** *119,* 551.
82. Sun, X.-Z.; George, M. W.; Kazarian, S. G.; Nikiforov, S. M.; Poliakoff, M. *J. Am. Chem. Soc.* **1996,** *118,* 10525.
83. (a) Hooker, R. H.; Mahmoud, K. A.; Rest, A. J. *J. Chem. Soc., Chem. Commun.* **1983,** 1022; (b) Hepp, A. F.; Blaha, J. P.; Lewis, C.; Wrighton, M. S. *Organometallics* **1984,** *3,* 174.
84. (a) Moore, B. D.; Simpson, M. B.; Poliakoff, M.; Turner, J. J. *J. Chem. Soc., Chem. Commun.* **1984,** 972; (b) Dixon, A. J.; George, M. W.; Hughes, C.; Poliakoff, M.; Turner, J. J. *J. Am. Chem. Soc.* **1992,** *114,* 1719.
85. Vitale, M.; Lee, K. K.; Hemann, C. F.; Hille, R.; Gustafson, T. L.; Bursten, B. E. *J. Am. Chem. Soc.* **1995,** *117,* 2286.
86. Hamaguchi, H.-o.; Gustafson, T. L. *Annu. Rev. Phys. Chem.* **1994,** *45,* 593.
87. Kitagawa, T.; Ogura, T. *Prog. Inorg. Chem.* **1997,** *45,* 431.
88. Schelvis, J. P. M.; Deinum, G.; Varotsis, C. A.; Ferguson-Miller, S.; Babcock, G. T. *J. Am. Chem. Soc.* **1997,** *119,* 8409.
89. Osman, R.; Pattison, D. I.; Perutz, R. N.; Bianchini, C.; Casares, J. A.; Peruzzini, M. *J. Am. Chem. Soc.* **1997,** *119,* 8459.
90. Colombo, M.; George, M. W.; Moore, J. N.; Pattison, D. I.; Perutz, R. N.; Virrels, I. G.; Ye, T.-Q. *J. Chem. Soc., Dalton Trans.,* **1997,** 2857.

91. Cheng, P. Y.; Zhong, D.; Zewail, A. H. *J. Chem. Phys.* **1996,** *105,* 6216.
92. Zhong, D.; Ahmad, S.; Zewail, A. H. *J. Am. Chem. Soc.* **1997,** *119,* 5978.
93. Stephens, J. W.; Morter, C. L.; Farhat, S. K.; Glass, G. P.; Curl, R. F. *J. Phys. Chem.* **1993,** *97,* 8944.
94. (a) Ischenko, A. A.; Schäfer, L.; Luo, J. Y.; Ewbank, J. D. *J. Phys. Chem.* **1994,** *98,* 8673; (b) Ischenko, A. A.; Ewbank, J. D.; Schäfer, L. *J. Phys. Chem.* **1995,** *99,* 15790.
95. (a) Williamson, J. C.; Zewail, A. H. *J. Phys. Chem.* **1994,** *98,* 2766; (b) Dantus, M.; Kim, S. B.; Williamson, J. C.; Zewail, A. H. *J. Phys. Chem.* **1994,** *98,* 2782.
96. Williamson, J. C.; Cao, J.; Ihee, H.; Frey, H.; Zewail, A. H. *Nature* **1997,** *386,* 159.
97. Turner, J. J.; George, M. W.; Johnson, F. P. A.; Westwell, J. R. *Coord. Chem. Rev.* **1993,** *125,* 101.
98. Perng, J.-H.; Zink, J. I. *Inorg. Chem.* **1990,** *29,* 1158.
99. Glyn, P.; Johnson, F. P. A.; George, M. W.; Lees, A. J.; Turner, J. J. *Inorg. Chem.* **1991,** *30,* 3543.
100. O'Hare, D. In "Inorganic Materials," 2nd ed. (D. W. Bruce and D. O'Hare, Eds.), Chap. 4, pp. 171–254, Wiley: Chichester, 1996.
101. (a) Šrajer, V.; Teng, T.-y.; Ursby, T.; Pradervand, C.; Ren, Z.; Adachi, S.-i.; Schildkamp, W.; Bourgeois, D.; Wulff, M.; Moffat, K. *Science* **1996,** *274,* 1726; (b) Eaton, W. A.; Henry, E. R.; Hofrichter, J. *Science* **1996,** *274,* 1631.
102. Clyne, M. A. A.; McKenney, D. J.; Watson, R. T. *J. Chem. Soc., Faraday Trans. 1* **1975,** *71,* 322.
103. Kukui, A.; Jungkamp, T. P. W.; Schindler, R. N. *Ber. Bunsenges. Phys. Chem.* **1994,** *98,* 1619.
104. Zagogianni, H.; Mellouki, A.; Poulet, G. *C. R. Acad. Sci. Paris, Ser. II* **1987,** *304,* 573.
105. (a) Ishiwata, T.; Tanaka, I.; Kawaguchi, K.; Hirota, E. *J. Chem. Phys.* **1985,** *82,* 2196; (b) Kawaguchi, K.; Hirota, E.; Ishiwata, T.; Tanaka, I. *J. Chem. Phys.* **1990,** *93,* 951.
106. Fujitake, M.; Hirota, E. *Spectrochim. Acta* **1994,** *50A,* 1345.
107. Bowers, C. P.; Fogelman, K. D.; Nagy, J. C.; Ridley, T. Y.; Wang, Y. L.; Evetts, S. W.; Margerum, D. W. *Anal. Chem.* **1997,** *69,* 431.
108. Liu, R. M.; McDonald, M. R.; Margerum, D. W. *Inorg. Chem.* **1995,** *34,* 6093.
109. Gazda, M.; Kumar, K.; Margerum, D. W. *Inorg. Chem.* **1995,** *34,* 3536.
110. Bourke, G. C. M.; Thompson, R. C. *Inorg. Chem.* **1987,** *26,* 903.
Rotzinger, F. P.; Grätzel, M. *Inorg. Chem.* **1987,** *26,* 3704.
111. Knoblowitz, M.; Morrow, J. I. *Inorg. Chem.* **1976,** *15,* 1674.
112. Moore, P. *Pure Appl. Chem.* **1985,** *57,* 347.
113. Brown, A. J.; Howarth, O. W.; Moore, P.; Parr, W. J. E. *J. Chem. Soc., Dalton Trans.* **1978,** 1776.
114. Dyson, H. J.; Wright, P. E. *Annu. Rev. Phys. Chem.* **1996,** *47,* 369.
115. Robinson, C. V.; Gross, M.; Eyles, S. J.; Ewbank, J. J.; Mayhew, M.; Hartl, F. U.; Dobson, C. M.; Radford, S. E. *Nature* **1994,** *372,* 646.
116. Hooke, S. D.; Eyles, S. J.; Miranker, A.; Radford, S. E.; Robinson, C. V.; Dobson, C. M. *J. Am. Chem. Soc.* **1995,** *117,* 7548.
117. (a) Armstrong, F. A.; Heering, H. A.; Hirst, J. *Chem. Soc. Rev.* **1997,** *26,* 169; (b) Heering, H. A.; Weiner, J. H.; Armstrong, F. A. *J. Am. Chem. Soc.,* **1997,** *119,* 11628.
118. (a) Crabtree, R. H. *Chem. Rev.* **1995,** *95,* 987; (b) Hall, C.; Perutz, R. N. *Chem. Rev.* **1996,** *96,* 3125.

119. (a) Bengali, A. A.; Arndtsen, B. A.; Burger, P. M.; Schultz, R. H.; Weiller, B. H.; Kyle, K. R.; Moore, C. B.; Bergman, R. G. *Pure Appl. Chem.* **1995,** *67,* 281; (b) Arndtsen, B. A.; Bergman, R. G.; Mobley, T. A.; Peterson, T. H. *Acc. Chem. Res.* **1995,** *28,* 154.

120. Müller, H. S. P.; Willner, H. *Inorg. Chem.* **1992,** *31,* 2527.